AMERICAN ACADEMY™ OF OPHTHALMOLOGY

Anatomic Clinical Trial Endpoints for Nonexudative Age-Related Macular Degeneration

Karen B. Schaal, MD, Philip J. Rosenfeld, MD, PhD, Giovanni Gregori, PhD, Zohar Yehoshua, MD, MHA, William J. Feuer, MS

Topic: To review the role of anatomic endpoints in clinical trials for the study of nonexudative age-related macular degeneration (AMD) with an emphasis on a novel composite endpoint for the study of emerging therapies for intermediate AMD (iAMD).

Clinical Relevance: Unlike clinical trials for exudative AMD, it is impractical to use the change in visual acuity (VA) as a primary endpoint for the study of nonexudative AMD. By the time VA has been lost in nonexudative AMD, proof-of-concept early-stage clinical trials would take years to run, and drug development would be a near impossible task. Surrogate endpoints are needed that reliably predict future vision loss and can be easily measured. Anatomic changes that correlate with disease progression in nonexudative AMD offer the greatest promise as primary endpoints.

Methods: In preparation for this review, the electronic PubMed database was searched for relevant research pertaining to anatomic endpoints for the study of nonexudative AMD. Paper selection was based on our knowledge of the field with the goal to be as inclusive as possible. Whenever possible, recent review articles and results from large clinical trials, preferably with outcomes from many years of follow-up were favored over trials of short duration.

Results: The most commonly used anatomic endpoint for the study of late, nonexudative AMD is the growth of geographic atrophy (GA). The advantages of studying GA include the appreciation that its enlargement through the foveal center leads to significant vision loss through the availability of natural history studies, the understanding that prevention of this growth would preserve vision in the future, the ability to reliably measure GA using different imaging strategies, and the development appropriate statistical tools that reliably predict the growth of GA over time. The major disadvantage of using GA is that significant, irreversible disease progression has already occurred. The use of drusen volume as a predictor of disease progression and the use of a composite endpoint that incorporates drusen growth, formation of GA, and formation of neovascularization offers an opportunity to study therapies at an earlier stage of AMD with a greater likelihood of preserving better vision over a lifetime.

Conclusions: Anatomic endpoints for the study of nonexudative AMD are needed to accelerate drug development, and the availability of optical coherence tomography algorithms capable of reliably measuring drusen morphology offer the best opportunity to study therapies for iAMD. *Ophthalmology 2016;123:1060-1079 © 2016 by the American Academy of Ophthalmology.*

Age-related macular degeneration (AMD) is a common, late-onset, slowly progressive, complex disorder responsible for irreversible blindness among the elderly worldwide.[1–3] The signs, symptoms, and clinical progression of AMD have been well described, and the most recent classification system separates AMD into 3 distinct stages: early, intermediate, and late.[4] The hallmarks of early AMD include medium-sized drusen ($\geq$63 and $<$125 μm) without pigmentary abnormalities. The features of intermediate AMD (iAMD) include large drusen ($\geq$125 μm) with or without pigmentary abnormalities or medium-sized drusen with pigmentary abnormalities. Late AMD is characterized by the presence of macular neovascularization (MNV) and/or geographic atrophy (GA) (Fig 1). In general, the term "nonexudative AMD" refers to all stages of early, intermediate, and late AMD that do not involve any neovascularization or exudation. When neovascularization arises in the setting of nonexudative AMD, the disease is then referred to as exudative AMD, but the underlying nonexudative AMD is still present and may progress unabated. Although neovascularization occurs in only 15% to 20% of patients with AMD, it has been the focus of most therapeutic interventions because of the rapid, sustained, and irreversible severe vision loss associated with neovascularization if left untreated. In contrast to exudative AMD, the vision loss associated with nonexudative AMD is more of a gradual process, taking years to progress.[5] With the successful development of drugs that inhibit vascular endothelial growth factor (VEGF), the rapid, severe vision loss from exudative AMD can be prevented. However, even with successful anti-VEGF therapy, patients continue to

http://dx.doi.org/10.1016/j.ophtha.2016.01.034
ISSN 0161-6420/16

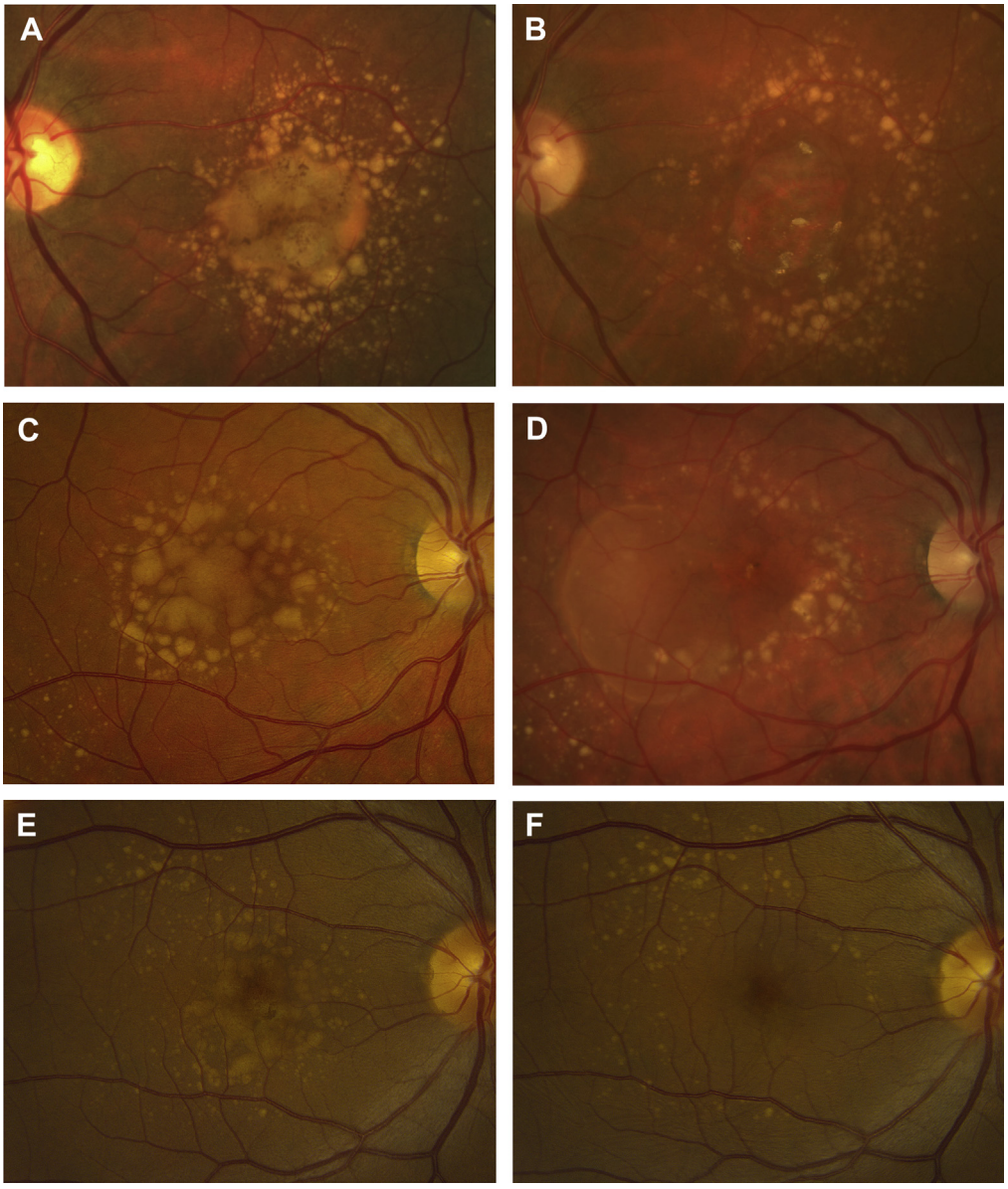

Figure 1. Color fundus images of 3 patients with intermediate age-related macular degeneration (AMD) showing disease progression and 3 different outcomes over time. **A**, **B**, Progression to geographic atrophy (GA) in the left eye of a 60-year-old man with large confluent drusen and pigmentary abnormalities in the central macula. After 3 years, drusen regression led to GA. **C**, **D**, Progression to macular neovascularization (MNV) in the right eye of a 74-year-old woman with large confluent drusen in the central macula. The drusen partially resolved, and the patient developed MNV in an area temporal to the fovea 4 years after first presentation. **E**, **F**, Drusen resolution without progression to late AMD in the right eye of a 61-year-old woman with large confluent drusen and pigmentary abnormalities in the central macula. Within 1 year after presentation, the drusen resolved without formation of MNV or GA (**F**).

slowly lose vision from the nonexudative disease, and macular atrophy often results after prolonged anti-VEGF therapy.[6–9] This macular atrophy can have an appearance similar to GA, and whether anti-VEGF therapy accelerates the formation or growth of GA remains controversial.

One strategy to improve long-term visual acuity outcomes when treating exudative AMD is to target additional pathways involved in the neovascular process. Another strategy, and perhaps an even better one, would be to stop or slow the underlying nonexudative AMD at an earlier stage when more visual acuity could be preserved. Promising therapies for nonexudative AMD are now being investigated, but to do so, it is necessary to design reliable clinical trials to test these novel therapies. Although the long-term goal of any treatment is to preserve vision, it is unrealistic to use visual acuity as a clinical trial endpoint in nonexudative AMD because vision loss takes many years to develop. This is a particular problem for early stage, proof-of-concept clinical trials in which it is impractical to use visual acuity as an endpoint and wait years to determine whether a treatment even seems to be effective so that longer, later-phase trials can be performed. For this reason,

there is a need to identify anatomic or surrogate endpoints that reflect disease progression and can reliably predict future vision loss, but can be studied over a shorter period of time.

The use of surrogate endpoints is known to have some significant limitations, but that has not prevented their use in ophthalmology, particularly in glaucoma clinical trials.[10] First, a surrogate outcome must be in the causal pathway from the point of intervention to the eventual outcome that is to be prevented. As in glaucoma, a surrogate outcome in the study of nonexudative AMD must be in the pathway leading to vision loss. The further removed the surrogate outcome is from the outcome that matters, the more chance there is for there to be a disconnect between the surrogate outcome and the meaningful one. Second, when considering a particular intervention, we must be confident that by measuring the effect on the surrogate outcome, we are capturing all the important effects of that intervention on the outcome of interest, which again is vision loss.[10] Also, when considering results, we are interested not only in whether an intervention alters a surrogate endpoint but also in the magnitude, precision, and duration of the effect. For example, if an intervention shows large reductions in the surrogate endpoint, if the 95% confidence intervals around those large reductions are narrow, and if the effect persists over a sufficiently long period of time, then our confidence increases that the desired outcome of preventing vision loss will be favorably affected. But, if the positive effects on the surrogate outcome are smaller, with wider confidence intervals, and of shorter duration, then we are less confident of the long-term effect on preventing vision loss. This review discusses the most practical, current anatomic endpoints for use in clinical trials designed to test promising therapies for nonexudative AMD.

Our search strategy was based on an electronic PubMed search in preparation for this review. Article selection was based on our knowledge of the field, with the goal to be as inclusive as possible. Whenever possible, recent review articles and results from large clinical trials, preferably with multiyear follow-up outcomes, were favored over research articles.

Part 1: Growth of Geographic Atrophy as an Anatomic Clinical Trial Endpoint

Imaging Geographic Atrophy and Comparison between Different Strategies

Currently, the most used clinical trial endpoint is to prevent or slow the development of GA over a defined period of time.[11,12] Because GA represents the loss of photoreceptors, retinal pigment epithelium (RPE), and choriocapillaris, and the development of GA correlates with the loss of vision due to the loss of photoreceptors, it stands to reason that the growth of GA through the foveal center would cause decreased central visual acuity. Thus, a treatment that prevents or slows the formation of central GA should delay the loss of central visual acuity better than no treatment at all. Regulatory authorities have accepted a slowing of enlargement of GA as a viable clinical trial endpoint. Currently, this endpoint is being used in clinical trials testing therapies for late nonexudative AMD.[5] However, the use of GA enlargement as a clinical trial endpoint requires extensive knowledge of the natural history and growth rate of GA so that biostatisticians can power clinical studies to detect a predetermined treatment effect, such as a slowing of the annual growth rate by 25%.

Four major imaging strategies have been used to document the formation and growth rate of GA: color fundus photography (CFP), fundus autofluorescence (FAF), fluorescein angiography, and spectral-domain optical coherence tomography (SD OCT)[13–20] (Fig 2). Historically, CFP was used to document the clinical features of AMD and to study disease progression in large population-based studies.[15,21–27] However, this imaging technique has difficulty identifying early GA and reliably establishing the margins of GA, resulting in only a moderate reproducibility rate when measuring the area of GA.[28,29] Despite these limitations, studies have reported that the mean rate of GA growth is between 1.2 and 2.8 mm^2/year.[5]

Holz and colleagues[5] studied the utility of FAF for measuring the growth of GA and for predicting progression rates on the basis of the surrounding patterns of abnormal hyperautofluorescence. In FAF imaging, the absence of a signal is assumed to correlate with the absence of the RPE. By repeatedly using FAF imaging to assess GA progression, this group found a median GA enlargement rate of 1.52 mm^2/year.[14] However, they also found that delineating the GA boundaries in the proximity of the foveal center could be difficult on FAF images because of the presence of retinal xanthophylls that absorb the excitation light (488 nm) and prevent the excitation of the lipofuscin within the underlying RPE. In addition, the presence of cataracts also limited image quality. Despite these limitations, and when using a semiautomated algorithm for detecting and measuring the size and progression of atrophic GA, Holz and colleagues[5] reported that their results were reproducible.[30]

More recently, questions have been raised about the assumption that the absence of autofluorescence truly represents a loss of RPE and that the presence of hyperautofluorescence represents RPE cells at risk of being lost.[31,32] Despite these concerns, the areas of hypofluorescence measured on FAF imaging and the location of RPE loss identified by Spectralis SD OCT B-scan imaging (Heidelberg Engineering, GmbH, Heidelberg, Germany) have shown good correlation.[33,34] However, foveal involvement was easier to assess using SD OCT imaging compared with FAF imaging.[34] Although similar in their overall assessment of GA area, SD OCT cross-sectional B-scan imaging has an added advantage of identifying anatomic abnormalities in the outer retina at the margins of GA, where photoreceptor abnormalities can precede the enlargement of GA and may serve as early indicators of disease progression.[16,33,35,36]

Spectral-domain optical coherence tomography (OCT) imaging identifies GA on the basis of the characteristic hypertransmission of light into the choroid below Bruch's membrane (BM) that occurs when the RPE is absent (Figs 2 and 3). This increased penetration of light into the choroid

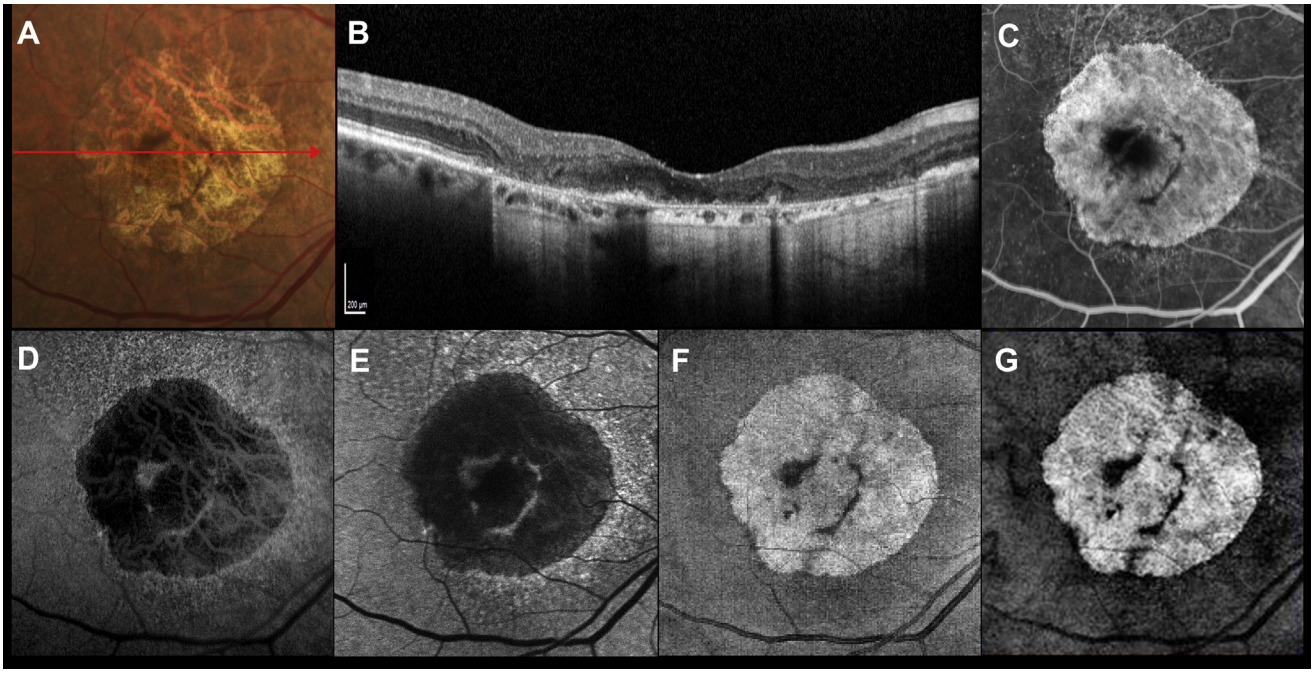

Figure 2. Right eye of an 83-year-old woman with central geographic atrophy (GA) secondary to age-related macular degeneration (AMD). The area of GA is visualized using different imaging strategies at the same visit. **A**, Color fundus photograph. **B**, Cross-sectional spectral-domain optical coherence tomography (OCT) B-scan that corresponds to the *red arrow* on the fundus photograph in **A**. **C**, Fluorescein angiography (Heidelberg Engineering, GmbH, Heidelberg, Germany). **D**, Topcon autofluorescence (Oakland, NJ). **E**, Heidelberg autofluorescence (Heidelberg Engineering, GmbH). **F**, An OCT fundus image, an en face projection of all the reflected light from all the A- and B-scans. **G**, An en face OCT projection of the reflected light from beneath the retinal pigment epithelium (RPE), known as the sub-RPE slab, with slab boundaries from 65 to 400 μm below the RPE.

occurs because the RPE and choriocapillaris, which normally scatter the light, are absent and their absence permits more light to penetrate into the choroid.[37,38] An added benefit of SD OCT imaging is that GA can be visualized using both cross-sectional B-scans and en face images from the same volume data set. En face visualizations generate a representation of the retina known as an "optical coherence tomography fundus image" (OFI). On OFIs, the atrophy appears brighter than the surrounding area because the en face image represents a summation of all the transmitted and reflected light from all the anatomic layers in each A-scan. If more light penetrates into the choroid at the location where the RPE and choriocapillaris are absent and then more light is reflected from the choroid back to the detector, then the atrophic area appears bright compared with the surrounding areas with intact RPE. The use of OFIs to detect and measure areas of GA has been shown to correlate well with GA detection on clinical examination, CFP, and FAF imaging.[13,20,37] Because of the reproducibility of GA measurements from OFIs, these OFIs can be used to follow the growth of GA and are at least as good or better than those obtained using CFP, FAF imaging, and fluorescein angiography.[17,29,39,40]

Another OCT-based en face imaging strategy for GA uses only the light that is reflected from the choroid beneath BM, rather than all the reflected light from a given A-scan (Fig 3). This technique generates so-called sub-RPE slab images, which are similar to OFIs but typically show higher contrast at the borders of GA.[41,42] Currently, the only fully automated, commercially available, Food and Drug Administration–approved algorithm for GA segmentation identifies GA from sub-RPE slab images (available on the Cirrus HD-OCT instrument; Carl Zeiss Meditec, Inc., Dublin, CA). These measurements have been compared with manual segmentation of GA and found to be in good agreement.[41]

Measuring the Growth of Geographic Atrophy and Strategies to Adjust for Baseline Variability in Size and Configuration

The OFIs were used to study the natural history of GA progression and determine the enlargement rate of GA.[13] When calculating the growth rate of GA, Yehoshua et al[13] found that using a square root transformation of the area had several advantages over using the area measurements themselves. The square root enlargement rates are computed as the difference between the square root of the area measurements at different time points. By using this strategy, they found that it was possible to eliminate the dependence of GA growth on baseline GA size.[13,43–46] This was an important development given the fact that previous observations had shown that the enlargement rates of GA depended on the baseline lesion size, with larger lesions growing faster.[14,15,17] Moreover, the standard deviation of the test–retest tolerance limits for a given measurement of GA area was found to increase as the lesion size increased, making statistical conclusions about progression

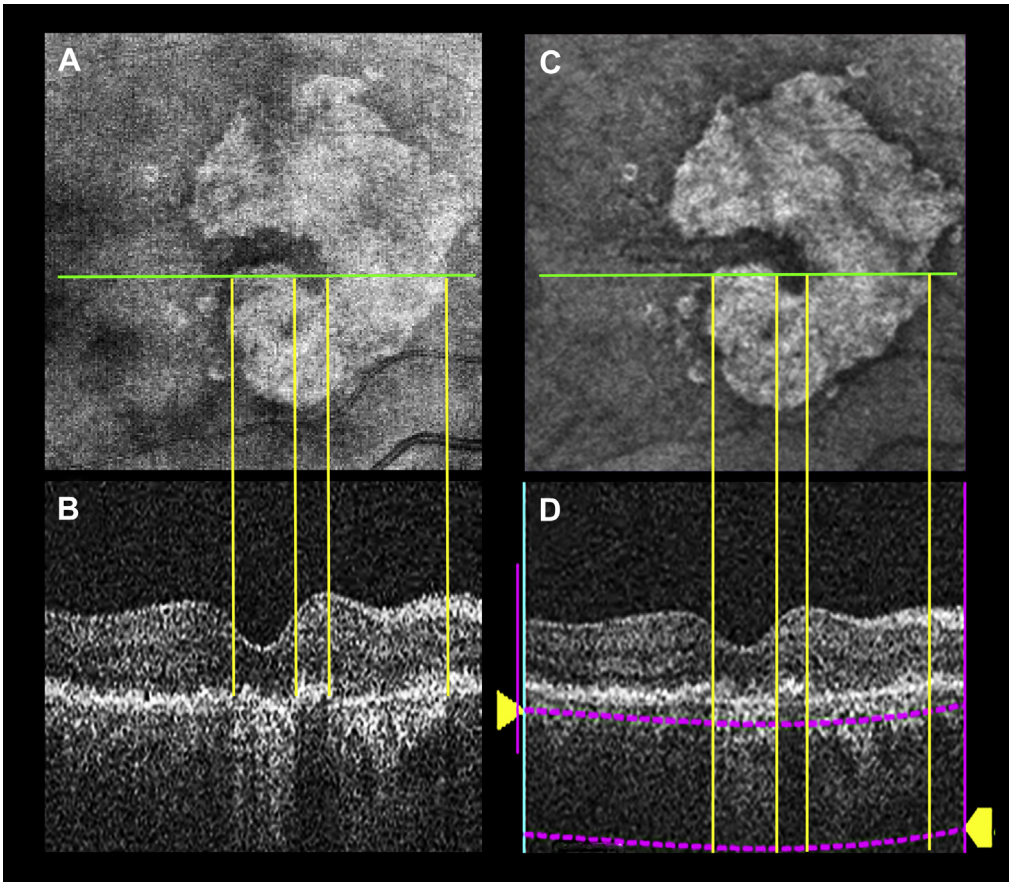

Figure 3. Right eye of a 90-year-old woman with geographic atrophy (GA) secondary to age-related macular degeneration (AMD). The areas of GA on the spectral-domain optical coherence tomography (OCT) en face images are correlated with the areas of hypertransmission on the corresponding cross-sectional B-scans. **A**, An OCT fundus image. **B**, Cross-sectional B-scan through the area of GA at the position indicated by the *green line* in **A**, demonstrating the increased signal in areas of retinal pigment epithelium (RPE) atrophy due to the hypertransmission into the choroid and increased choroidal reflectance. **C**, En face slab from beneath the RPE derived from the area between the *magenta dotted lines* in **D**. **D**, Cross-sectional B-scan through the same area of GA as indicated by the *green line* in **A**, indicating the slab boundaries used to generate the sub-RPE slab in **C** (65–400 μm below the RPE).

difficult. By using the square root strategy, they found an overall median growth rate of 0.26 mm/year for all lesions. Multifocal lesions were shown to grow faster, with a median growth rate of 0.30 mm/year, compared with unifocal lesions that had a median growth rate of 0.15 mm/year. This statistically significant difference ($P = 0.001$) was apparent only when the square root transformation strategy was applied to lesion area measurements.

The advantages of using a square root transformation strategy were validated by an analysis of the original Age-Related Eye Disease Study (AREDS) data.[17] Feuer et al[43] showed that by using the square root transformation, the original dependence of the growth rate on the baseline lesion size was eliminated[43] (Fig 4). Moreover, they found that very small lesions and very large lesions grew more slowly than lesions between 0.5 and 7 disc areas in size, which is consistent with clinical experience.[43] After all, the normal enlargement of GA never continues until it occupies the entire posterior pole of an eye. The usefulness of the square root transformation was confirmed in the Comparison of AMD Treatments Trial.[9] Grunwald et al[9] used digital color photographs and fluorescein angiograms at baseline and at 1 and 2 years to determine the growth rate of GA. Three approaches for modeling GA growth were undertaken: (1) total GA area without transformation, (2) square root transformation, and (3) log transformation. The square root transformation strategy was shown to be the best at eliminating the growth rate dependence on baseline lesion size and was used for all subsequent analyses. Among 194 eyes evaluable for growth, GA growth rate was determined to be 0.43 mm/year.

The use of the square root transformation simplifies the design and enrollment of clinical trials by eliminating the need to specify a narrow range of lesion sizes or to adjust for baseline lesion sizes in the primary outcome analysis. Because the growth rate of GA is constant between the sizes of 0.5 and 7 disc areas, this represents a broad range of lesion sizes that can be included in clinical studies designed to test the effect of treatments on the growth rate of GA. Furthermore, the square root transformation strategy produces uniform test–retest tolerance limits. As a result, fewer patients need to be enrolled compared with the number of patients who would be needed in studies using standard area measurements.[13]

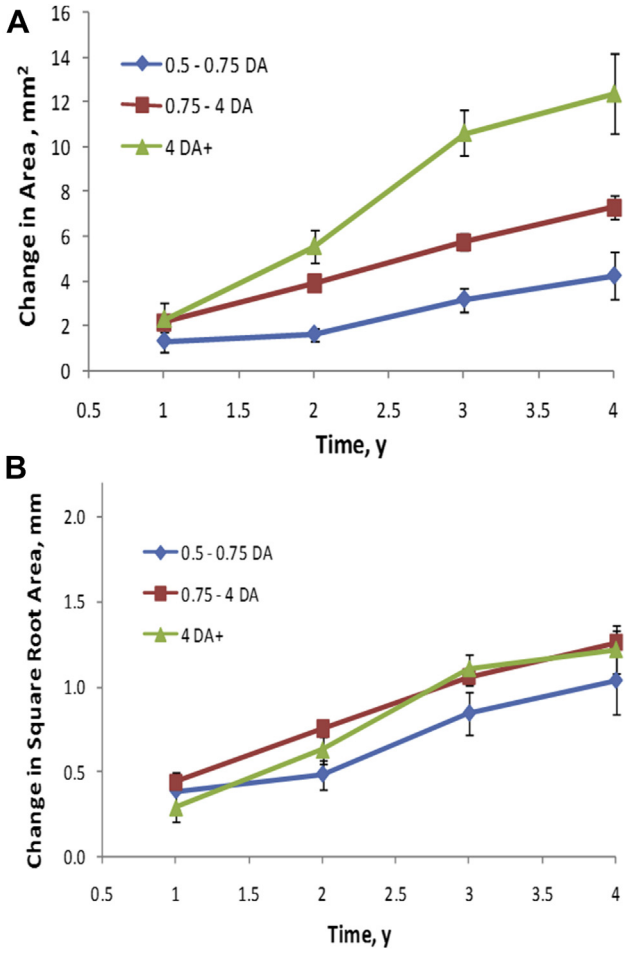

Figure 4. Change in the area of geographic atrophy (GA) by baseline lesion size calculated using the differences in (**A**) the standard area measurements (**B**) and the square root of these area measurements using data from the Age-Related Eye Disease Study (AREDS) Report No. 26. **A**, Original analysis showing the change in area over 4 years for each of the baseline lesion size categories. **B**, Revised analysis showing the change in the square root of the area measurements for each of the baseline lesion size categories. The graphs demonstrate that after applying the square root transformation strategy, the growth of GA no longer is dependent on baseline lesion size. This strategy has proven useful in designing trials to evaluate drug effects on GA growth rates. DA = disc area. (Figure from Feuer et al.[43])

One advantage of SD OCT en face imaging is that it can be used to assess the integrity of different retinal layers around the entire perimeter of GA, which can help predict GA growth. Nunes et al[45] identified photoreceptor outer segment abnormalities along the margins of GA by using a 20-μm−thick SD OCT en face slab that included the inner segment/outer segment band, also known as "band #2" or the "ellipsoid zone." They found that abnormalities in this slab extended over a thousand microns from certain margins of the GA. These findings were consistent with the observations of Bird et al,[47] who performed a histopathologic review of autopsy eyes with AMD and GA and reported outer retinal photoreceptor abnormalities extending large distances from certain margins of GA. Nunes et al[45] found that in some eyes, these areas of ellipsoid zone disruption identified by SD OCT en face imaging were predictive of where the GA would enlarge over the ensuing year (Fig 5). Stetson et al[46] used another SD OCT en face imaging strategy to predict the margin of GA that was most likely to enlarge. This strategy used a minimum-intensity algorithm to create an en face image that represented the minimum-intensity signal from each A-scan. In healthy retina, the minimum intensity (darkest signal) from each OCT A-scan is localized within the outer nuclear layer. However, the minimum intensity along the margin of GA was found to be typically higher, presumably because of some disruption of the photoreceptors. Photoreceptor disruption was visualized using this en face minimum-intensity slab projection image and correlated with areas where the GA would progress.

Another important feature of GA that needs to be taken into account when evaluating its growth rate is the shape of the GA. Irregularly shaped GA has been shown to grow faster than circularly shaped, unifocal GA. These areas of irregularly shaped GA are known as "multilobular GA." Another configuration of GA that has been shown to grow faster is multifocal GA, which is GA comprising multiple discrete foci. A circularity index (CI) has been proposed to help explain these growth differences.[48] The CI is the ratio of the actual total lesion area with a given perimeter over the area of a circular lesion with the same perimeter. They found that lesions with a smaller CI value, or lesions that were less circular, tended to grow faster. To simplify their findings, they categorized CI values into 3 groups: 0.25 (very irregular), 0.25 to <0.75 (partly irregular), and ≥ 0.75 (circular), and the mean ($\pm$ standard deviation) growth rates in these 3 groups using the square root transformation strategy were 0.40 (± 0.18), 0.36 (± 0.30), and 0.21 (± 0.22) mm/year, respectively ($P < 0.001$).[48] This strategy is complicated by the fact that lesions continually change shape and coalesce as the disease progresses, so a baseline CI value may change over time.

Current Clinical Trials Using Growth of Geographic Atrophy as a Primary Clinical Trial Endpoint

Current and past clinical trials have explored the growth of GA as an anatomic endpoint to test whether therapies slow the enlargement of GA.[5] Previously, AREDS used CFP to investigate whether zinc and antioxidants could slow the progression of GA; no treatment effect was found. Likewise, no slowing of GA was detected in the ciliary neurotrophic factor implant trial[49] (ciliary neurotrophic factor/NT501; Neurotech Pharmaceuticals, Cumberland, RI), the topical OT-551 trial[50] (a disubstituted hydroxylamine with antioxidant properties; Othera Pharmaceuticals, Conshohocken, PA), the oral fenretinide trial[51] (a serum retinol-binding protein antagonist; Sirion Therapeutics, Tampa, FL), the subconjunctival sirolimus trial[52] (rapamycin; Santen Pharmaceuticals, Osaka-shi, Japan), and the Complement inhibition with eculizumab for the treatment of nonexudative age-related macular degeneration (COMPLETE) study,[44] which evaluated eculizumab (Soliris; Alexion Pharmaceuticals, Cheshire, CT), a systemic

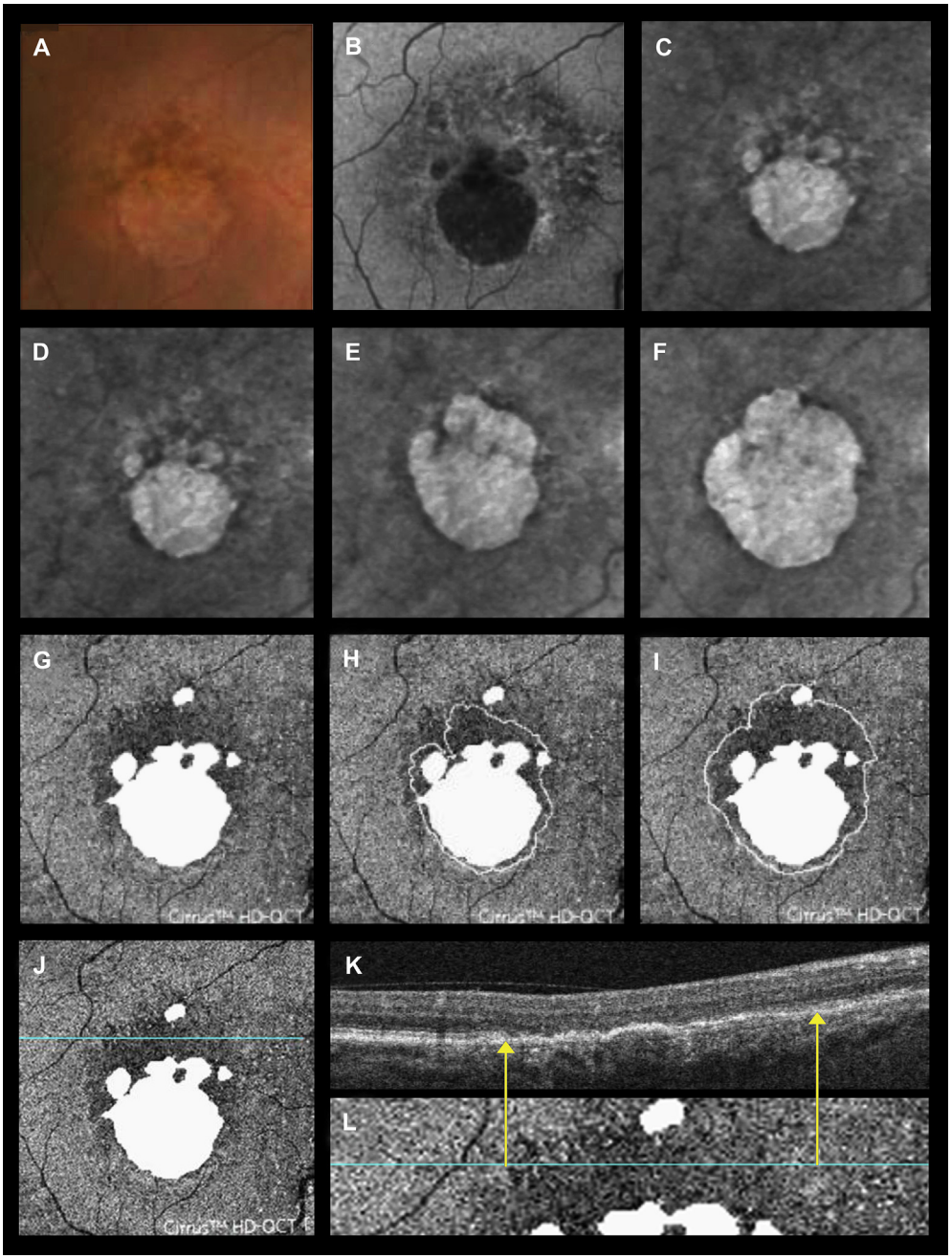

Figure 5. Progression of geographic atrophy (GA) predicted by en face imaging of the outer retina and disruption of photoreceptors. Right eye of an 80-year-old man with GA secondary to age-related macular degeneration (AMD) visualized with different imaging modalities and followed over time. Outer retinal slab images help to predict the edge of GA at risk for progression. **A**–**C**, Different imaging modalities at the same visit used to show the area of GA. **A**, Color fundus image at baseline showing central GA. The size of the color image represents the area scanned with spectral-domain optical coherence tomography (OCT) imaging. **B**, Fundus autofluorescence (FAF) corresponding to the area shown in **A**. **C**, En face OCT imaging of the light reflected from 65 to 400 μm beneath the sub–retinal pigment epithelium (RPE) slab corresponding to the area shown in **A** and **B**. **D**–**F**, Sub-RPE slabs showing GA growth over time. **D**, Baseline visit (same image as **C**). **E**, Week 26 visit. **F**, Week 60 visit. **G**–**I**, Baseline outer retinal en face slab images with slab boundaries located 20 to 40 μm above the RPE. The *white area* of GA at baseline (**C**, **D**) is superimposed on the en face outer retinal slabs. **G**, Baseline outer retinal en face slab with superimposed baseline area of GA (*white*). **H**, Outline showing the growth of GA at week 26, with the baseline area of GA in *white*. **I**, Outline showing the growth of GA at week 60, with the baseline area of GA in *white*. **J**–**L**, Correlation between an individual B-scan and the pattern observed on the outer retinal en face slab. **J**, Baseline en face outer retinal slab with superimposed baseline area of GA (same image as **G**) and a *blue line* indicating the location of the B-scan shown in **K**. **K**, Cross-sectional spectral-domain OCT B-scan through the area of reduced intensity at the location of the blue line shown in **J**. **L**, Magnified image section from image **J**. *Yellow arrows* show the correlation between the area of reduced (dark) intensity on the en face slab and the outer retinal disruption on the B-scan. (Figure modified from Nunes et al.[45])

complement factor 5 inhibitor. The COMPLETE study is the only trial so far that used SD OCT en face imaging and the square root transformation strategy to assess the growth rate of GA.[44] To date, the only trial that has demonstrated a slowing of GA growth is the MAHALO study, which explored monthly intravitreal injections of the complement factor D inhibitor known as "lampalizumab." This slowing of the GA growth rate was observed only in a genetic subgroup of patients carrying a particular complement factor I at-risk allele (rs17440077) (Genentech/Roche, South San Francisco, CA). A larger confirmatory phase II/III trial is currently under way using lampalizumab. Additional ongoing trials using beta-amyloid inhibitors, visual cycle modulators, and complement inhibitors may yet demonstrate a definitive treatment effect in slowing the enlargement of GA. However, it is entirely possible that GA may be too late in the disease process to demonstrate a significant treatment effect, and it may be necessary to intervene at an earlier stage before GA develops. Moreover, even if a drug is effective in slowing the growth of GA, it may be even more effective if used earlier in the disease process by preventing the formation of GA and preserving even more vision over a lifetime. For these reasons, it is a priority to develop clinical trial endpoints that can be used at an earlier stage of AMD.

Part 2: Progression of Drusen as an Anatomic Clinical Trial Endpoint

Classification of Drusen

Drusen are one of the earliest signs of AMD. They appear as yellow-white deposits on biomicroscopic examination and color fundus imaging.[4] Histopathologic studies have shown that drusen are focal accumulations of extracellular material (mainly lipids and proteins), typically located between the basal lamina of the RPE and the inner collagenous layer of BM. Drusen have been classified by their greatest diameter, such as in small (<63 μm), intermediate (≥63 but <125 μm), and large (≥125 μm); by their appearance, such as hard and soft drusen; and by their borders, such as in distinct or indistinct. Drusen are dynamic structures; they can increase in size, coalesce, or regress. When regressing, they usually lead to GA or MNV.[53] On rare occasions, they can regress without any obvious sequelae. Drusen characteristics are important for staging the severity of AMD and for predicting the likelihood of disease progression. Soft, large, indistinct, and confluent drusen present the greatest risk for progression to late AMD (GA, MNV, or both).[54–56]

Staging of Age-Related Macular Degeneration: Location, Distribution, and Appearance of Drusen

Currently, several AMD grading and classification systems, as well as severity scales, have been developed in an effort to provide standards for clinicians and researchers in the diagnosis and management of AMD.[54,57–61] A simplified (basic) AMD clinical classification system was introduced as a consensus agreement based on the scientific literature and expert opinions.[4] To make it suitable for worldwide use, this system requires only the use of biomicroscopy. This basic AMD classification system focuses on the development of large drusen and pigmentary abnormalities within 2 disc diameters of the fovea. Drupelets (small drusen <63 μm in diameter) were considered a consequence of normal aging and are not part of the AMD classification system. Early AMD was defined by medium-sized drusen (≥63 but <125 μm), and eyes with medium-sized drusen require monitoring because of the known risk of progression to late AMD, which is defined as GA, MNV, or both. An even greater likelihood of progression to late AMD was found with any drusen ≥63 μm in size associated with definite hyperpigmentation or hypopigmentation. Moreover, for persons with medium drusen in only 1 eye, the 5-year risk of progression to large drusen is approximately 25%, and for those with medium drusen in both eyes, the 5-year risk of progression to large drusen is more than 50%. These large drusen (≥125 μm in the smallest diameter) have been associated with an even greater likelihood of disease progression to late AMD. A simplified 5-step severity scale based on drusen size and pigmentary changes was developed to help predict the likelihood of progression from intermediate to late AMD.[4,59] Of note, population-based studies also observed that drusen could spontaneously regress without any residual sequelae. Over a period of 15 years, 18% of soft indistinct drusen were found to regress without leaving any traces.[57] Other studies have reported that 20% to 34% of drusen disappeared over 5 to 7 years.[62,63] This phenomenon of drusen disappearance without sequelae would be a particularly desirable outcome in a clinical trial if the goal were to prevent or slow further disease progression.

Role of Drusen as Risk Factors for Progression to Late Age-Related Macular Degeneration: Use of Color Fundus Imaging to Quantitate Drusen

Drusen need to be graded and quantified to assess the risk of developing late AMD. Most of the grading and classification systems for AMD are based on standardized grading of color fundus images. Over the past few decades, manual grading of stereoscopic high-quality color fundus images was the gold standard and was used in large epidemiologic studies such as AREDS.[22] Different grading systems for drusen quantification using stereoscopic color fundus images have been validated, such as the Wisconsin grading system, the International Classification system, and the AREDS classification system.[64] They all use circles of standard radii centered on the fovea, but they vary in how they subdivide the macula into areas of interest and how they assess drusen size, type, area, confluence, and associated pigmentary alterations.

Although manual grading of drusen has proven to be useful, it is time-consuming and costly, and the results can vary because of the ambiguity of drusen appearance, media opacities, image quality, and interpatient fundus pigmentation. Even experienced graders are challenged when using color images to grade drusen. This led to the introduction of semiautomated and automated algorithms in an attempt to standardize and facilitate drusen quantification using digital

fundus photographs.[64–68] Unfortunately, the numbers of drusen counted by automated thresholding techniques were shown to differ significantly from the gold standard of manually counting drusen. Overall, attempts at automated drusen segmentation using color images have shown variable degrees of robustness and accuracy, and none of these techniques have gained widespread acceptance nor have they been incorporated as an outcome measure in large clinical trials.

Optical Coherence Tomography and Quantitation of Drusen

Spectral-domain OCT has greatly enhanced our ability to morphologically assess drusen. High-speed, high-density, and high-resolution SD OCT scans of the macula have been used to characterize the 2- and 3-dimensional features of drusen, and both volume and area measurements can be calculated using automated algorithms. Not only can drusen be visualized using both B-scans and topological maps, but also the integrity of the overlying retina can be visualized in great detail. As a result, the impact of drusen morphology on the overlying photoreceptors can be assessed. More important, the integrity of the RPE can be followed as the disease progresses, and focal RPE changes, pigment clumps, and GA can be identified more easily.

The information about drusen that can be extracted from SD OCT is different and complementary to the information obtained from color fundus imaging (Fig 6). Although color fundus imaging lacks any information about the 3-dimensional morphology of drusen, such as their volume and position relative to the RPE, SD OCT can differentiate between typical drusen, which are drusen located below the RPE, and subretinal drusenoid deposits or reticular pseudodrusen, which are accumulations of material underneath the retina and above the RPE.[69–72] In CFP, drusen are defined in terms of changes in macular pigmentation, usually clinically detectable once they reach 25 to 30 μm in diameter. In SD OCT, drusen typically present as accumulations of material underneath the RPE and lead to deformation of overlying RPE.[73] For these typical drusen, SD OCT can provide reliable volume measurements above a minimal size threshold.[74] Spectral-domain OCT also is useful for looking at changes within

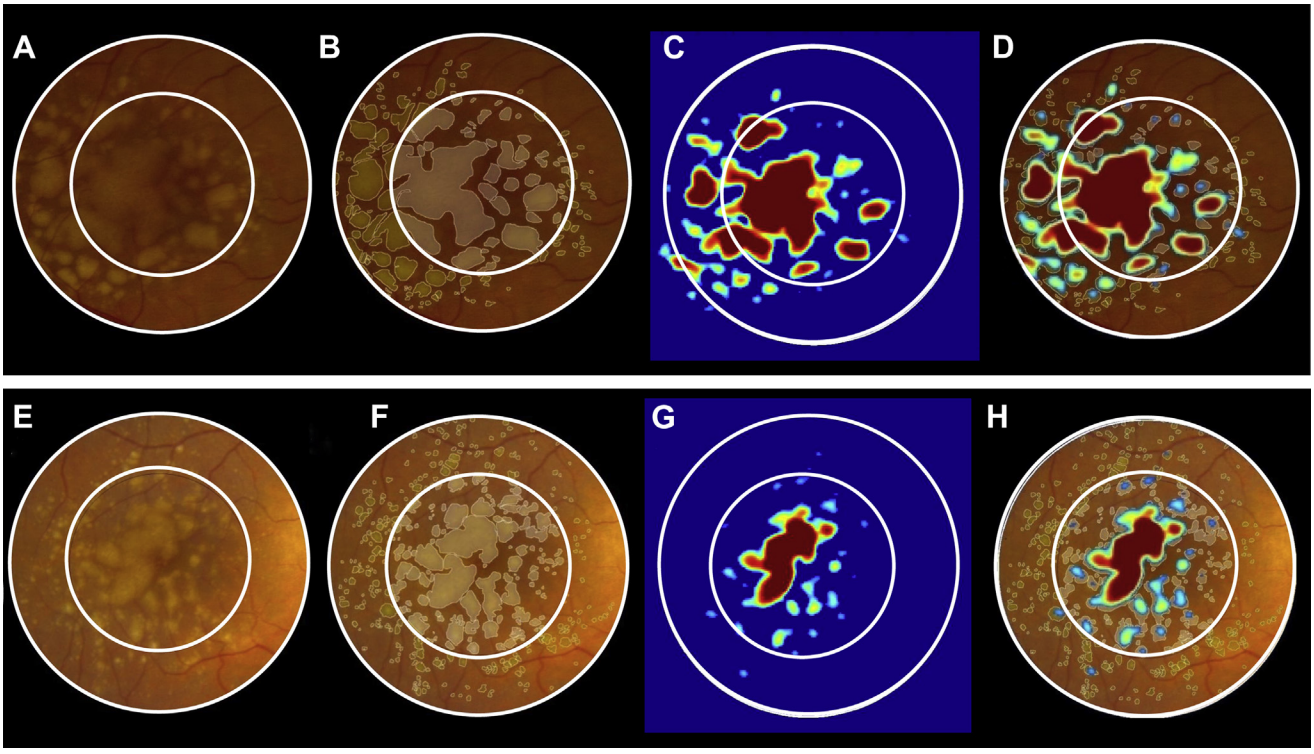

Figure 6. Comparison between manual drusen measurements on color fundus images and automated drusen measurements using spectral-domain optical coherence tomography (SD OCT). **A–D**, Examples of good agreement between drusen areas manually outlined on color fundus images and automatically measured by the SD OCT algorithm. **A**, Color fundus image with 3- and 5-mm circular overlays centered on the fovea. **B**, Drusen manually outlined by the reading center (drusen area 3.46 mm^2 [3-mm circle], 5.65 mm^2 [5-mm circle]). **C**, Drusen map obtained using the automated SD OCT algorithm (drusen area 3.47 mm^2 [3-mm circle], 5.14 mm^2 [5-mm circle]). **D**, Overlay of the automated and manual drusen maps showing good agreement, although the SD OCT algorithm did not identify all of the hypopigmented areas on the color fundus image outlined as drusen by the graders. **E–H**, Example of larger drusen area measured manually from the color fundus image compared with the automated SD OCT algorithm. **E**, Color fundus image with 3- and 5-mm circular overlays centered on the fovea. **F**, Drusen manually outlined by the reading center (drusen area 3.03 mm^2 [3-mm circle], 4.13 mm^2 [5-mm circle]). **G**, Drusen map from SD OCT with the 3- and 5-mm circles centered on the fovea (drusen area 1.85 mm^2 [3-mm circle], 1.88 mm^2 [5-mm circle]). **H**, Overlay of the automated and manual drusen maps showing that the SD OCT algorithm did not identify the majority of the small hypopigmented areas on the color fundus image outlined as drusen by the graders. (Figure modified from Yehoshua et al.[81])

individual drusen, within the retina, and within the choroid that may be predictive of disease progression. For example, the presence of heterogeneous internal reflectivity in drusenoid lesions and hyperreflective foci overlying drusen in the retina were found to be associated with an increased risk of local atrophy.[75] Moreover, OCT features within the retina have been identified that uniquely predict the formation of drusen-associated atrophy.[76] These changes, known as "nascent GA," include a subsidence of the outer plexiform layer and inner nuclear layer, with the development of a hyporeflective wedge-shaped band within the limits of the outer plexiform layer.[76] These OCT findings in conjunction with the hypertransmission of light into the choroid are characteristics of nascent GA and not detectable on color fundus imaging.

Different SD OCT algorithms have been developed by different research groups to quantify the drusen load in the macula.[74,77–79] Several of these algorithms have been compared with color fundus imaging. A fully automated algorithm is now commercially available on the Cirrus HD-OCT (Carl Zeiss Meditec Inc.). This algorithm generates drusen volume and area measurements on the basis of the quantitative assessment of RPE deformations,[74] and it has been shown to reliably follow drusen morphologic changes over time.[80] The general strategy used by the algorithm involves calculating the difference between the elevation of the RPE caused by drusen and a virtual RPE floor free of deformations. Such algorithms necessarily require a balance between precision and reproducibility. In particular, a minimum height threshold of 10 pixels (19.5 μm) is used to assess drusen. Deformations below this threshold cannot be distinguished successfully from the noise associated with a measurement and are not included as part of the volume measurement.

Comparing Drusen Measurements from Color Fundus Images and Spectral-Domain Optical Coherence Tomography Images

A comparison between drusen area measurements manually outlined from color fundus photos and the fully automated SD OCT algorithm showed only fair agreement.[81] Measurements of drusen on color fundus images typically were larger than those on OCT images (Fig 6). This difference in measurements resulted from the underlying difference in the definition of drusen. The SD OCT algorithm tended to overlook lesions that do not lead to significant elevation of the RPE, such as small, flat drusen and subretinal drusenoid deposits. Conversely, not all deformations in the RPE geometry seen on SD OCT correlate with obvious pigmentary changes on color fundus imaging.[74] Despite the fact that it might underestimate small, shallow drusen, the OCT algorithm worked well for medium-sized and larger drusen, which are widely recognized as risk factors for progression to late AMD and are clinically more meaningful when assessing disease severity and likelihood of disease progression.[19] Although drusen area measurements using SD OCT images tended to be systematically smaller than drusen area measurements using color fundus images, SD OCT drusen assessments were highly reproducible and easier to perform in the clinic, without the need for reading center involvement and certified graders.[80] Moreover, SD OCT can be used to measure both the volume and the area of drusen. Although there was a good correlation between area and volume measurements, area measurements tended to plateau as the drusen volume grew larger over time, and drusen volume was shown to be a more sensitive indicator of drusen growth.[80] Of note, when considering the change of drusen area over time, there was no significant difference between the color fundus imaging and SD OCT strategies.[80] This suggested that both modalities essentially capture the same changes in drusen area and can be explained by the observation that most of the changes in drusen area are due to morphologic changes of large soft drusen, which also cause deformation of the RPE and are captured with both imaging modalities. Although changes in drusen area may not differ between color fundus imaging and SD OCT, it is possible for drusen volume, as measured by SD OCT, to decrease by more than 50% of the cube root volume without any apparent change in drusen area using color fundus imaging.[53] The cube root transformation of drusen volume measurements has the same desirable properties as the square root transformation of GA area measurements.[74]

Another study compared drusen measurements obtained using the automated drusen segmentation algorithm on the Cirrus HD-OCT instrument with drusen measurements obtained by manual grading of color fundus and infrared retromode images.[82] The use of retromode produced a pseudo 3-dimensional image, and drusen appeared as raised structures with more clearly defined boundaries, which facilitated their detection. They also found that the drusen number measured by SD OCT was significantly smaller than the number measured by manual segmentation on color fundus images. However, the mean drusen area measurements from SD OCT did not differ significantly from the mean drusen area measurements obtained from the planar fundus images. The difference between this study and the previous study comparing color fundus imaging and SD OCT measurements of drusen can be explained by the difference in distribution of drusen types between the 2 studies, with larger drusen resulting in better correlations between the 2 imaging modalities. Overall, SD OCT area measurements of drusen were found to be more precise compared with measurements from color fundus images, and these measurements were more sensitive to the underlying changes in drusen morphology such as volume.

Quantitative characteristics of drusen detected automatically from Cirrus SD OCT scans have been examined to estimate the likelihood of disease progression from early and iAMD to MNV.[83] Drusen characteristics (number, extent, area, volume, shape, density, and reflectivity) were automatically extracted from the data sets and followed over a period of 5 years. Area, volume, height, and reflectivity of drusen were found to be informative features that distinguished between cases that progressed and did not progress. However, the most significant predictor for progression within 30 months was the total drusen volume from the SD OCT data sets. In another study, Nathoo et al[84]

confirmed an association between the drusen load, measured as area or volume (determined using automated SD OCT measurements), and the development of late AMD.

In a study from Duke University, drusen measurements were compared between color fundus images and SD OCT data sets, and most of the disagreements were found at the margins of drusen.[85] This quantitative comparison used an SD OCT semiautomated segmentation algorithm known as the "Duke OCT Retinal Analysis Program." They found a trend toward greater detection of larger drusen with SD OCT and a trend toward greater detection of small, hard drusen with color fundus imaging. The inability to detect small drusen with the SD OCT algorithm was explained to be possibly a result of the spacing used between adjacent B-scans, which were set at 66-μm intervals. When areas with drusen on color fundus imaging and areas with drusen on SD OCT were compared pixel by pixel, they found an 82% agreement between the 2 modalities. A more recent article from this group reported on the predictive value of the Duke OCT Retinal Analysis Program in a population of patients with iAMD from the AREDS2 study.[78] A greater baseline drusen volume was predictive of an increased 2-year progression to neovascularization, and an abnormal thinning of the RPE–drusen complex at baseline was associated with a higher incidence of GA after 2 years. Once again, the quantitative assessment of drusen was shown to be predictive of disease progression.

Although reading centers have developed proprietary algorithms for drusen detection, 3 commercially available SD OCT instruments currently offer this capability. In a report describing segmentation algorithms for the detection of drusen, results of drusen detection using the Cirrus HD-OCT, the 3DOCT-1000 (Topcon, Tokyo, Japan), and the Spectralis instruments (Heidelberg Engineering, GmbH, Heidelberg, Germany) were compared.[86] Every druse in each B-scan was identified and graded by 2 independent expert graders and compared with automated segmentation of the RPE performed by the SD OCT instruments. The segmentation algorithm used in the Cirrus instrument was the best-performing algorithm when the 200×200 raster scan was used. By using the Cirrus, the investigators reported that 30% of the identified drusen were detected with negligible errors, whereas the 3DOCT-1000 algorithm detected only 8.6% of the drusen with negligible error. Overall, the automated segmentation of the RPE by Cirrus made significantly fewer errors in detecting drusen than the 3DOCT-1000 ($P < 0.001$). It was predominantly the large drusen, >300 μm in diameter, that were delineated correctly. The Spectralis instrument performed poorly because its software did not offer true segmentation of the RPE.

Another strategy for segmenting and quantifying drusen in AMD uses a prototype polarization-sensitive (PS) OCT.[87] The algorithm segments the RPE on the basis of its depolarizing properties.[88] To estimate the potential of PS OCT for quantitative assessment of drusen size and total area in patients with early AMD, the authors compared drusen segmented by the automated algorithm and analyzed with PS OCT with drusen detected by manual segmentation of each individual B-scan.[89] A 512×128 raster scan pattern covering an area of 6×6 mm was used. The automated segmentation algorithm identified 96.5% of all drusen without significant error, and the number of detected drusen was significantly larger with automated rather than manual segmentation. In general, PS OCT segmentation was superior to color fundus imaging, with only 10% of all small drusen (i.e., drusen <63 μm in diameter) missed by the algorithm. Although this imaging strategy may be useful, it is experimental and not widely available at this time.

Clinical Trials for Intermediate Age-Related Macular Degeneration

Intermediate AMD is defined by the presence of large drusen (≥125 μm) or medium-sized drusen associated with any pigmentary abnormalities.[4] If this stage could be arrested or the progression to late AMD (MNV and GA) slowed or prevented, then there would be a greater chance of preserving better long-term vision compared with initiating treatment once late AMD arises. However, to test therapies for iAMD, it is necessary to design clinical trials that demonstrate a slowing of disease progression. Because iAMD is characterized by the presence of drusen and pigmentary abnormalities, it stands to reason that these features need to be included in any evaluation of a clinical trial endpoint. However, before any clinical trial can be designed to test a therapy that alters normal disease progression in eyes with iAMD, it is necessary to understand the natural history of iAMD. In the past, the natural history of iAMD has been studied using color fundus imaging, but now SD OCT offers a more reliable imaging strategy for quantifying drusen and following their progression (Fig 7). Moreover, OCT is more sensitive and accurate in detecting both MNV and GA compared with color fundus imaging alone.

With the ability of SD OCT to assess elevations of the RPE, drusen volume, drusen area, reflectivity of drusen contents, changes in drusen ultrastructure,[90] and changes in adjacent retinal anatomy,[91] it is reasonable to assume that SD OCT could be superior to CFP for following disease progression and identifying potential anatomic endpoints. To understand the natural history of drusen and disease progression using SD OCT, Yehoshua et al[53] followed drusen secondary to AMD over a period of 24 months and quantified volumetric changes in drusen using Cirrus SD OCT imaging. Drusen volume and drusen area were measured within circular regions measuring 3 and 5 mm in diameter centered on the fovea. Cube root and square root transformations were used for drusen volume and drusen area, respectively. This is analogous to the square root transformation used for the area of GA and establishes a constant test–retest tolerance limit for drusen measurement that is independent of baseline drusen size.[74] Drusen volume was designated as having increased or decreased if a follow-up measurement was outside the 95% test–retest tolerance limits from the baseline measurement. The study found that drusen volume on average grew larger over time, and there was an increased likelihood that the larger drusen

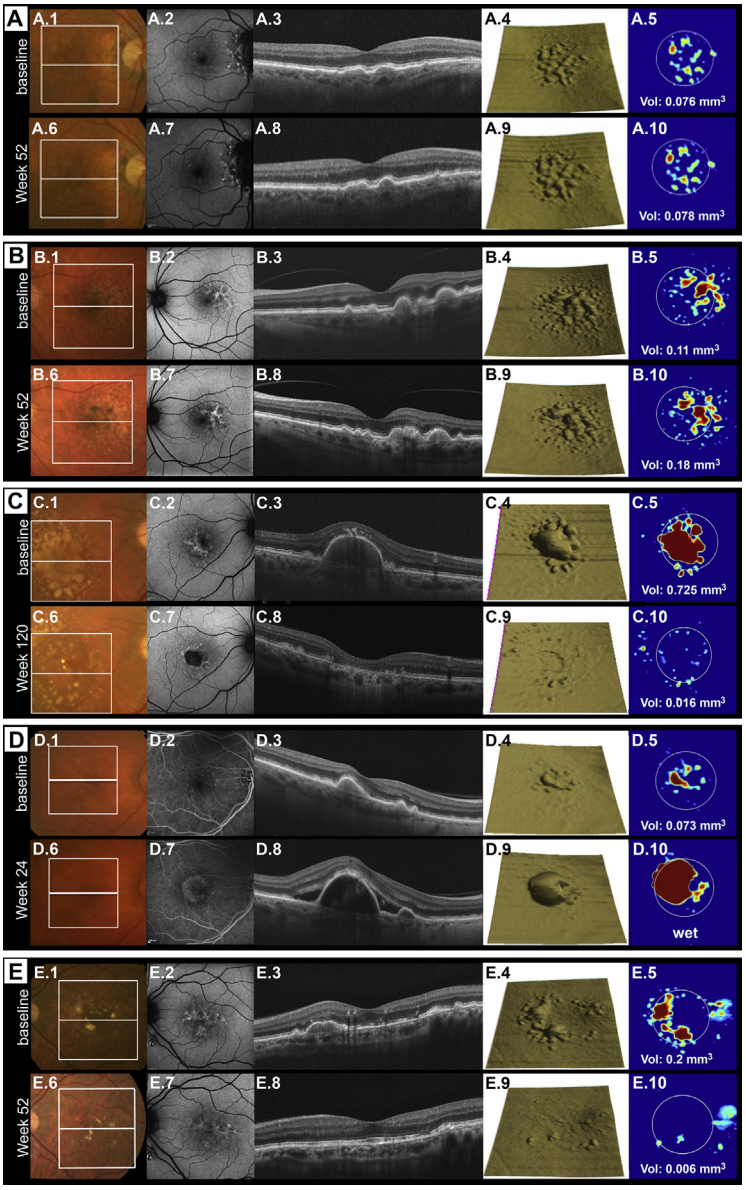

Figure 7. Intermediate age-related macular degeneration (AMD) and normal disease progression documented using color fundus imaging, autofluorescence imaging, spectral-domain optical coherence tomography (SD OCT), and drusen volume assessment. *White boxes* on the color fundus images (**A.1**, **A.6**, **B.1**, **B.6**, **C.1**, **C.6**, **D.1**, **D.6**, **E.1**, **E.6**) indicate the area scanned with SD OCT. The *white circle* on the drusen volume maps (**A.5**, **A.10**, **B.5**, **B.10**, **C.5**, **C.10**, **D.5**, **D.10**, **E.5**, **E.10**) represent a 3-mm area centered on the fovea. Drusen volume measurements within this 3-mm circle are depicted on the panels. **A**, Right eye of a 79-year-old man with stable drusen volumes over 52 weeks. **A.1**—**A.5**, Baseline visit. **A.6**—**A.10**, Week 52 visit. **A.1**, **A.6**, Color fundus images. **A.2**, **A.7**, Autofluorescence images. **A3**, **A.8**, Cross-sectional optical coherence tomography (OCT) B-scans at the position marked by the *horizontal white line* on **A.1** and **A.6**. **A.4**, **A.9**, A retinal pigment epithelium (RPE) segmentation map. **A.5**, **A.10**, Drusen volume maps within a 3-mm area centered on the fovea. **B**, Left eye of a 72-year-old man with an increase in drusen volume over 52 weeks. **B.1**—**B.5**, Baseline visit. **B.6**—**B.10**, Week 52 visit. **B.1**, **B.6**, Color fundus images. **B.2**, **B.7**, Autofluorescence images. **B.3**, **B.8**, Cross-sectional OCT B-scans at the position marked by the *horizontal white line* on **B.1** and **B.6**. **B.4**, **B.9**, Retinal pigment epithelium segmentation maps. **B.5**, **B.10**, Drusen volume maps within a 3-mm area centered on the fovea. **C**, Right eye of a 61-year-old man who progressed to geographic atrophy (GA) over a course of 120 weeks. **C.1**—**C.5**, Baseline visit. **C.6**—**C.10**, Week 120 visit. **C.1**, **C.6**, Color fundus images. **C.2**, **C.7**, Autofluorescence images. **C.3**, **C.8**, Cross-sectional OCT B-scans at the position marked by the *horizontal white line* on **C.1** and **C.6**. **C.4**, **C.9**, Retinal pigment epithelium segmentation maps. **C.5**, **C.10**, Drusen volume maps within a 3-mm area centered on the fovea. **D**, Right eye of a 75-year-old woman with macular neovascularization (MNV) developing 24 weeks after her first presentation. **D.1**—**D.5**, Baseline visit. **D.6**—**D.10**, Week 24 visit. **D.1**, **D.6**, Color fundus images. **D.2**, **D.7**, Fluorescein angiography images showing no MNV at baseline (**D.2**) and well-delineated MNV at week 24 (**D.7**). **D.3**, **D.8**, Cross-sectional OCT B-scans at the position marked by the *horizontal white line* in **D.1** and **D.6**. **D.4**, **D.9**, Retinal pigment epithelium segmentation maps. **D.5**, **D.10**, Drusen volume maps within a 3-mm area centered on the fovea, with **D.10** showing the volume of the vascularized RPE detachment. **E**, Left eye of a 61-year-old man with a decrease in drusen volume over 52 weeks. **E.1**—**E.5**, Baseline visit. **E.6**—**E.10**, Week 52 visit. **E.1**, **E.6**, Color fundus images. **E.2**, **E.7**, Autofluorescence images. **E.3**, **E.8**, Cross-sectional OCT B-scan at the position marked by the *horizontal white line* on **E.1** and **E.6**. **E.4**, **E.9**, Retinal pigment epithelium segmentation maps. **E.5**, **E.10**, Drusen volume maps within a 3-mm area centered on the fovea.

would decrease or collapse over time. An analysis of the eyes in which drusen volume regressed significantly during follow-up showed that 64% of the eyes progressed to GA, 23% of the eyes progressed to MNV, and 14% of drusen regressed without any residual retinal abnormalities based on SD OCT (Fig 7). It was noticed that drusen can go through repeated cycles of growth and shrinkage, with growth more likely than shrinkage, and this undulating behavior of drusen seemed to be more dependent on their baseline volume rather than the duration of follow-up. These observations were consistent with previous studies that reported an increased risk of progression to MNV or GA with larger drusen areas at baseline.[4,92,93] However, Yehoshua et al[53] showed that SD OCT was better at picking up the subtlety of how drusen morphology undulated over time compared with color fundus imaging. In fact, drusen volume measured by SD OCT could decrease by more than 90% without any apparent change on the corresponding color fundus images.[53]

Another strategy for following drusen on SD OCT was reported by Ouyang et al.[75] Using the Spectralis SD OCT instrument (Heidelberg Engineering, Vista, CA), they assessed longitudinal changes in drusen features for a minimum of 6 months and evaluated maximum lesion height and diameter, lesion internal reflectivity, presence and extent of overlying intraretinal hyperreflective foci, and choroidal thickness both subfoveally and below drusen. The presence of hyperreflective foci overlying the drusen, heterogeneous internal reflectivity of drusen, or choroidal thickness less than 135 μm below the drusen at baseline was noted to increase the risk of local atrophy.

Decrease in Drusen Volume as a Clinical Trial Endpoint

The goal of any treatment for iAMD should be to alter the expected disease progression. Natural history studies have shown that as drusen enlarge, they are more likely to progress to GA or MNV. It is also possible for drusen to spontaneously disappear without any obvious sequelae, and this outcome has been reported in association with different interventions. The application of laser photocoagulation,[94,95] rhegmatogenous retinal detachment,[96] pars plana vitrectomy,[97,98] and anti-VEGF therapy[99] have been reported to be associated with the resolution of drusen after treatment. Whether drusen resolution would result in a long-term positive effect on disease progression remains a controversial topic, but the idea of modifying a feature of iAMD already associated with a high risk of disease progression is an attractive strategy. Critics of such a strategy would argue that drusen are not responsible for disease progression, but rather are a sign of disease, and their resolution would not alter the inexorable progression to late AMD. This cause-and-effect controversy is similar to the associations that have been drawn between beta-amyloid plaques in the brains of patients with Alzheimer disease and disease progression. As in Alzheimer disease, the controversy surrounding whether the resolution of the drusen would alter normal disease progression awaits treatments capable of eliminating drusen and a study design that appropriately follows disease progression. Because drusen resolution is a rare occurrence, it is a particularly attractive clinical trial endpoint because it would not take many patients to show a therapeutic success for a study with a duration as short as 6 months.[53] Currently, there are 2 broad strategies to help facilitate drusen resolution: laser therapy and pharmacotherapy.

Laser-for-Drusen Trials

On the basis of the clinical observation that drusen could resolve after laser treatment, laser photocoagulation for drusen was investigated worldwide to prevent disease progression to late AMD.[94] In the randomized, controlled trials of laser therapy of drusen, the primary outcome measure was to prevent the progression to MNV or GA. Drusen reduction and visual acuity were considered secondary endpoints. All the clinical trials recruited patients with medium (≥63 μm, <125 μm) or large (≥125 μm) drusen and pigmentary changes, but the studies were otherwise different, with a variety of different treatment strategies. Laser parameters varied between the studies, and spot sizes ranged from 50 to 200 μm, burn durations ranged from 0.05 to 0.2 seconds, and number of laser spots ranged from 1 to 60. The types of lasers included argon laser, yellow laser, and diode laser, including subthreshold photocoagulation (810-nm diode laser). Overall, according to a Cochrane review of this topic,[94] these trials were considered to represent a moderate quality of evidence because of certain limitations, such as poorly defined enrollment criteria, lack of masked patients, lack of masking of visual acuity examiners in more than half of the studies, lack of power to assess endpoints, and the failure to draw appropriate conclusions. This Cochrane review planned to evaluate drusen reduction by considering eyes that had at least a 50% reduction in drusen area from baseline using stereoscopic color photographs, but this outcome was assessed in only a few studies. Because of lack of data, the review was altered to allow reports based on the investigators' definition. The Choroidal Neovascularization and Prevention Trial found a drusen reduction of 50% or more in 83% of treated eyes compared with 45% of control eyes at 18 months. The Prophylactic Treatment of AMD study reported an apparent drusen reduction in 50% of treated eyes compared with less than 1% of control eyes, and the Complications of Age-Related Macular Degeneration Prevention Trial found a drusen reduction of at least 50% in 34.3% treated eyes versus 8.6% control eyes at 2 years (1008 subjects). However, the results of the Cochrane meta-analysis indicated that prophylactic laser treatment of drusen, although drusen reduction occurred, was not effective in delaying AMD progression and in preventing vision loss, and is therefore not recommended. However, all of these studies failed to take into account the central drusen burden within the macula, the impact of this drusen load on visual acuity before and after laser therapy, and the presence of macular atrophy and its impact on visual acuity. Moreover, OCT was not available when these studies were performed.

Next-Generation Laser-for-Drusen Trials: Nanosecond Laser Treatment for Intermediate Age-Related Macular Degeneration

A minimally destructive nanosecond laser was used for the treatment of iAMD, and because of the low energy profile associated with this new laser, retinal damage should be minimal.[100,101] The goal of this ultra-low-energy laser with a wavelength of 532 nm (3ns, 2RT laser; Ellex, Adelaide, SA, Australia) was to deliver subthreshold energy to the retina in which the laser power was titrated to be below a visual threshold for retinal change in each eye (range, 0.15−0.45 mJ). A change in drusen area was assessed on the basis of color fundus imaging, and the percentage of drusen area was calculated within specific regions (5 concentric circles, each divided into 4 quadrants). A decrease in drusen area was defined as a decrease of >5% of the baseline drusen area.[100] Patients received 12 laser spots (400-μm spot diameter) in a single session evenly distributed around the macula at a safe distance (>500 μm) from the fovea. This single nanosecond laser treatment was reported to lead to a decrease in drusen area in approximately 40% of patients with iAMD, and approximately 75% of treated eyes showed no change in the FAF pattern at 2 years, indicating that the laser treatment did not promote GA. Of note, significant drusen regression also was observed in the nontreated fellow eye at 1 year. The exact mechanism of this effect is not yet fully understood. Automated drusen volume calculation with the Cirrus SD OCT was performed only in a subgroup of patients because the device was not available at the beginning of the study.[101] When using the automated drusen volume calculation, the proportion of participants with drusen volume reduction was significantly higher compared with natural history data.

The effect of the nanosecond laser on the retina and RPE and the laser's effect on retinal microglia were assessed histopathologically in mice and 2 human eyes.[100] The 2 individuals treated with the laser were diagnosed with a lid malignancy, and nanosecond laser was applied before the scheduled enucleation. For both humans and mice, a well-defined laser injury at the level of the RPE monolayer was noticed, and cells of mononuclear origin were evident on the distal regions of the photoreceptor outer segments after treatment. The mouse model showed enhanced cell proliferation at the border of the laser defect, and over time, enlarged RPE cells filled in the defect with preservation of the overlying retinal layers. In the mouse model, gene expression of extracellular matrix proteins was altered in the treated study eyes and nontreated fellow eyes, and key RPE genes were unchanged. Furthermore, enhanced microglial surveillance (not activation) and unchanged complement factor 3 levels were found in the mouse model. To study the effect of laser therapy on the early histopathologic changes typical in AMD, such as a thickened BM, the investigators treated an apolipoprotein E null mouse model with a thickened BM, and after a single nanosecond laser session, the BM thickness was reduced by 23% across the retina, not only in the treated areas. This nanosecond laser therapy for drusen is now being studied in a large, multicenter, randomized clinical trial: the Laser Intervention in Early Age-Related Macular Degeneration Study (ClinicalTrials.gov identifier: NCT01790802).

Next Generation Laser-for-Drusen Trials: Sublethal Laser Treatment for Intermediate Age-Related Macular Degeneration

More recently, a nondamaging laser therapy for the retina has been introduced using Endpoint Management (EpM) with the PASCAL Streamline 577 nm laser system (Topcon Medical Laser Systems, Inc., Santa Clara, CA).[102,103] A titration protocol with a computational model−based algorithm for adjustment of laser power and duration was used to find the energy level that did not result in any tissue damage.[103] The titration protocol was calibrated in rabbits and begins with laser power settings that result in a barely visible burn. This laser power, at a 20-ms pulse duration, was defined as 100%. All other pulse energies were expressed as a percentage of this titration threshold. At 50% to 75% energy levels, lesions typically were not visible on fundus examination but were detectable with fluorescein angiography and SD OCT. Histopathologic examination showed that the damage was confined primarily to the RPE with minor effects on photoreceptors. The lesions produced using 30% to 50% laser power were invisible on OCT, FAF, and fluorescein angiography, and the damage was limited primarily to the RPE and observed using scanning electron microscopic imaging. The laser power at the 30% level had no evidence of retinal damage, and was therefore considered to be nondamaging and photo-stimulating. This was confirmed using both light microscopy and transmission electron microscopy, which did not reveal any visible damage in the retina or RPE and even showed normal RPE cells in the center of the laser spot. The EpM laser settings were first used clinically for the treatment of patients with chronic central serous chorioretinopathy.[102] The hypothesized mechanism of action using EpM laser is thought to be due to the upregulation of heat shock proteins after the photo-stimulation of RPE. Heat shock proteins are responsible for protein quality control by refolding damaged proteins, and they protect cells from protein aggregation, proteotoxicity, and apoptosis. One hypothesis is that heat shock proteins can help rejuvenate cellular functions. The effect of using the EpM laser on drusen volume in eyes with iAMD measured with the Cirrus HD-OCT algorithm is being investigated in an ongoing clinical trial (ClinicalTrials.gov identifier: NCT02569892).

Change in Spectral-Domain Optical Coherence Tomography Drusen Volume as a Clinical Trial Endpoint

The use of SD OCT to assess drusen volume in the central macula has been shown to provide a reliable and reproducible method for measuring the morphology of drusen over time.[53,74,104] The software for measuring drusen volume is Food and Drug Administration approved and commercially available on the Cirrus HD-OCT instrument. The change in drusen volume as a clinical trial endpoint for studying a therapy for nonexudative AMD was first used in

the COMPLETE study.[104] The COMPLETE study was a 12-month, investigator-sponsored, single-center, prospective, randomized, double-masked trial designed to evaluate the safety and efficacy of intravenous eculizumab (a complement C5 inhibitor) for the treatment of patients with drusen secondary to AMD. The primary outcome was to determine whether the treatment with eculizumab could decrease the cube-root volume of drusen volume by at least 50% within a 3-mm circle centered on the fovea over a 6-month treatment period. Such a decrease in drusen cube-root volume, without evidence of progression to GA or MNV, constituted a successful outcome.

In the COMPLETE study, the reduction in drusen volume was chosen as a surrogate anatomic endpoint because it could be studied over a shorter period of time compared with other nonexudative AMD efficacy endpoints, such as the progression to late AMD or vision loss. This anatomic endpoint allowed the investigators to design a short proof-of-concept study. Because a dramatic change in drusen volume was a rare, spontaneous occurrence, and when it did happen, it occurred over a period of weeks rather than years, it stands to reason that a useful anatomic endpoint to test new therapies could be a decrease in drusen volume. If a therapy could dramatically decrease drusen volume, then the study would require fewer subjects and a shorter duration compared with studies using endpoints that occurred more frequently and more slowly, such as the onset or enlargement of GA. If eculizumab could dramatically decrease drusen volume, then this would be sufficient evidence to commit to a larger study to demonstrate that eculizumab could modify long-term disease progression.

In the COMPLETE study, eyes with a baseline drusen volume of 0.03 mm^3 or greater and without any GA were treated for 6 months and then observed for 6 months. A drusen volume of $\geq$0.03 mm^3 (cube-root volume 0.31 mm) was chosen on the basis of a natural history study of eyes with this drusen volume.[53] This volume always corresponded to iAMD with large drusen ($\geq$125 μm), and this volume could be measured reliably with SD OCT. Moreover, a decrease of 50% in this drusen volume using the cube-root transformation strategy could be measured reliably as well, and this cube-root decrease corresponds to an 88% decrease using standard volume measurements. Thus, a baseline drusen volume $\geq$0.03 mm^3 was considered suitable as a baseline volume when studying therapies for iAMD. In the COMPLETE study,[105] the proportion of eyes at follow-up with decreasing, stable, and increasing drusen volumes were 20%, 26%, 54%, respectively (Fig 7), which were the outcomes predicted from the previous natural history study.[53] However, in the COMPLETE study, there was no statistically significant effect of eculizumab on drusen volume.

An interesting outcome of the COMPLETE study was that the growth of drusen volume over 6 months seemed to depend on the number of complement factor H (CFH) at-risk alleles carried by the patients. In as few as 30 patients, we showed a statistically significant difference in the rate at which the drusen volume increased, with drusen volume growing fastest in subjects with 2 at-risk CFH alleles. This increase was detected as early as 6 months into the study and maintained through the last follow-up (12 months). A recent study of an Amish population with AMD confirmed this association between the area and volume of macular drusen as assessed by SD OCT and the number of CFH at-risk alleles carried by subjects.[106] The number of CFH at-risk alleles carried by the patient was shown to influence the size and volume of drusen in these Amish patients. These observations supported the association between the number of disease-associated alleles carried by the patient and the disease severity as determined by drusen size measurements obtained using SD OCT.

Another noteworthy outcome of the COMPLETE study was that 2 of the 10 placebo-treated patients progressed to MNV, whereas none of the 20 actively treated patients progressed. Although this difference was not statistically significant, this outcome raised the question of whether MNV might have been prevented if more patients had been enrolled in the study or the enrolled patients had been followed longer. This outcome also raised the possibility of using a clinical trial endpoint that focuses more on preventing drusen progression rather than on promoting drusen regression because prevention of disease progression might be an easier outcome to achieve than drusen regression. If a therapy could prevent drusen growth and the progression of drusen to both GA and MNV, then the therapy could prevent or delay the onset of late AMD and preserve more vision than a treatment that just slows the enlargement of GA. Thus, it became apparent that SD OCT assessment of drusen volume was useful for 2 possible clinical trial endpoints in studying iAMD. The first endpoint was the reduction of drusen volume without progression to GA or MNV, and the second endpoint was the prevention of drusen growth without progression to GA or MNV. By combining the prevention of drusen growth without the formation of MNV or GA into 1 summary composite endpoint that represented prevention of disease progression, we were able to develop a clinical trial design with smaller sample sizes, shorter study duration, and lower study costs than studies using the traditional visual acuity endpoint.[107] Because any effective treatment for iAMD should prevent drusen growth, formation of GA, and formation of MNV from occurring, we propose the use of this composite endpoint in future clinical trials designed to test therapies for iAMD. This composite endpoint uses the 3 most likely outcomes when following eyes with iAMD. If we assume, on the basis of our previous research, a cumulative incidence of MNV at 1 year of 4.5%, a cumulative incidence of GA at 1 year of 5.0%, and the likelihood of drusen growth at 1 year of approximately 50%, then we can design a composite clinical trial endpoint in which the goal of treatment is to prevent the 60% likelihood of normal disease progression. For example, to design a study with 90% power to detect a 50% decrease in the failure rate at 1 year, that is, a decrease from 60% to 30% using the composite endpoint, only 62 subjects would be needed in each group assuming a 1:1 randomization between drug and placebo[104] (Table 1).

The use of composite endpoints in clinical trials carries risks, especially when the purpose of creating one is to increase the event rate in the control group with a view to

Table 1. Number of Subjects to Be Included in Each Arm of a Study Designed to Test a Therapy to Prevent Disease Progression for Intermediate Age-Related Macular Degeneration

Power of Study to Detect Treatment Effect	No. of Subjects Needed for Each Treatment Group According to the Predicted Percentage of Failures in Actively Treated Group at 1 Year*			
	50% Decrease in Failure Rate (30% Failure Rate)	*75% Decrease in Failure Rate (15% Failure Rate)*	*92% Decrease in Failure Rate (5% Failure Rate)*	*98% Decrease in Failure Rate (1% Failure Rate)*
80%	48	21	13	11
90%	62	26	16	14

*Based on an estimated failure rate of 60% in the placebo group based on natural history data and 1:1 randomization in the clinical trial. Failure was defined as an increase in drusen volume, formation of neovascularization, or formation of geographic atrophy at 1 year.

decrease the sample size necessary to obtain adequate statistical power.[108] Considerations that must be kept in mind when assessing the components of such an endpoint include their relative frequencies, their relative importance to patients, and the relative efficacy of the study intervention among them. Our proposed endpoint is made up of components with unequal frequencies, and they are not of equal importance. However, our aim in combining them was not to increase the event rate. The principal outcome of interest, and by far the most common one, is drusen volume increase. We also include progression to GA or MNV to ensure that these more serious natural history outcomes are captured in the analysis. Trials based on this composite endpoint should scrutinize separately the influence of the study intervention on GA and MNV, the direct precursors to vision loss, although the power to detect efficacy differences between components is apt to be low.

Summary of Anatomic Clinical Trial Endpoints in Nonexudative Age-Related Macular Degeneration

Prevention of disease progression is the primary objective of any study testing a novel therapy for nonexudative AMD. However, to design clinical trials, it is first necessary to understand normal disease progression. In AMD, as drusen area and volume increase, early AMD progresses to iAMD, which then leads to GA or MNV, the anatomic characteristics of late AMD. One strategy being used to alter disease progression in nonexudative AMD is to treat GA in the hope of slowing its growth rate. To date, the only therapy that has demonstrated any evidence of a treatment benefit has been intravitreal injections of a complement factor D inhibitor known as lampalizumab. However, this effect was observed only in a genetic subgroup of eyes with GA and has not yet been replicated. Although most studies have targeted the slowing of GA growth, it is important to consider the possibility that GA may be too late in the disease process for any drug to dramatically demonstrate a long-term visual acuity benefit. After all, slowing the growth of GA still results in the loss of photoreceptors at the margins of GA, albeit at a slower pace. Therefore, it stands to reason that treating earlier in the disease process and slowing its natural history would result in even greater preservation of vision as the patient ages. Moreover, the pathologic processes responsible for disease progression starting with iAMD may be different than the processes responsible for the development of GA in late AMD. Thus, a therapy that is effective in slowing the development of GA in late AMD may or may not have a benefit if used earlier in the disease process, and a therapy that is unsuccessful or marginal in slowing GA development may have a far greater benefit if used earlier in the disease. For these reasons, it is essential to develop clinical trial endpoints that can be used at an earlier stage of AMD, such as iAMD.

Drusen are the earliest signs of AMD and are the hallmark of early and iAMD. The advent of SD OCT imaging of drusen, its ability to characterize drusen morphology, and the development of algorithms to reliably quantify drusen volume and area have resulted in a new strategy for designing clinical trials starting with iAMD. With the increased sensitivity of SD OCT, it is now possible to consider interventions and clinical trial designs for iAMD that are more efficient and require fewer patients and shorter duration compared with previous trials based on color fundus imaging. Whether it is a study looking at laser therapy for drusen or a drug therapy, the ideal population of patients to study has a baseline drusen volume of $\geq$0.03 mm^3 in the absence of any signs of GA. An appropriate transformation, such as cube root in the case of drusen volume, should be used to analyze the results and evaluate drusen growth. In designing a trial starting with iAMD and a drusen burden of at least 0.03 mm^3, we propose the use of an anatomic composite endpoint with failure defined as drusen growth, formation of MNV, or formation of GA. If designed correctly, then a phase II study to test the efficacy of a treatment for iAMD could be performed with approximately 120 study participants over a period as short as 6 months to 1 year.

References

1. Klein R, Klein BE, Linton KL. Prevalence of age-related maculopathy. The Beaver Dam Eye Study. Ophthalmology 1992;99:933–43.
2. Pascolini D, Mariotti SP. Global estimates of visual impairment: 2010. Br J Ophthalmol 2012;96:614–8.

3. Friedman DS, O'Colmain BJ, Munoz B, et al. Prevalence of age-related macular degeneration in the United States. Arch Ophthalmol 2004;122:564–72.
4. Ferris FL 3rd, Wilkinson CP, Bird A, et al. Clinical classification of age-related macular degeneration. Ophthalmology 2013;120:844–51.
5. Holz FG, Strauss EC, Schmitz-Valckenberg S, van Lookeren Campagne M. Geographic atrophy: clinical features and potential therapeutic approaches. Ophthalmology 2014;121:1079–91.
6. Chakravarthy U, Harding SP, Rogers CA, et al. Alternative treatments to inhibit VEGF in age-related choroidal neovascularisation: 2-year findings of the IVAN randomised controlled trial. Lancet 2013;382:1258–67.
7. Rosenfeld PJ, Shapiro H, Tuomi L, et al. Characteristics of patients losing vision after 2 years of monthly dosing in the phase III ranibizumab clinical trials. Ophthalmology 2011;118:523–30.
8. Grunwald JE, Daniel E, Huang J, et al. Risk of geographic atrophy in the comparison of age-related macular degeneration treatments trials. Ophthalmology 2014;121:150–61.
9. Grunwald JE, Pistilli M, Ying GS, et al. Growth of geographic atrophy in the comparison of age-related macular degeneration treatments trials. Ophthalmology 2015;122:809–16.
10. Medeiros FA. Biomarkers and surrogate endpoints in glaucoma clinical trials. Br J Ophthalmol 2015;99:599–603.
11. Yehoshua Z, Rosenfeld PJ, Albini TA. Current clinical trials in dry AMD and the definition of appropriate clinical outcome measures. Semin Ophthalmol 2011;26:167–80.
12. Csaky KG, Richman EA, Ferris FL 3rd. Report from the NEI/FDA Ophthalmic Clinical Trial Design and Endpoints Symposium. Invest Ophthalmol Vis Sci 2008;49:479–89.
13. Yehoshua Z, Rosenfeld PJ, Gregori G, et al. Progression of geographic atrophy in age-related macular degeneration imaged with spectral domain optical coherence tomography. Ophthalmology 2011;118:679–86.
14. Holz FG, Bindewald-Wittich A, Fleckenstein M, et al. Progression of geographic atrophy and impact of fundus autofluorescence patterns in age-related macular degeneration. Am J Ophthalmol 2007;143:463–72.
15. Sunness JS, Margalit E, Srikumaran D, et al. The long-term natural history of geographic atrophy from age-related macular degeneration: enlargement of atrophy and implications for interventional clinical trials. Ophthalmology 2007;114:271–7.
16. Fleckenstein M, Schmitz-Valckenberg S, Adrion C, et al. Tracking progression with spectral-domain optical coherence tomography in geographic atrophy caused by age-related macular degeneration. Invest Ophthalmol Vis Sci 2010;51:3846–52.
17. Lindblad AS, Lloyd PC, Clemons TE, et al. Change in area of geographic atrophy in the Age-Related Eye Disease Study: AREDS report number 26. Arch Ophthalmol 2009;127:1168–74.
18. Schutze C, Ahlers C, Sacu S, et al. Performance of OCT segmentation procedures to assess morphology and extension in geographic atrophy. Acta Ophthalmol 2011;89:235–40.
19. Diniz B, Rodger DC, Chavali VR, et al. Drusen and RPE atrophy automated quantification by optical coherence tomography in an elderly population. Eye (Lond) 2015;29:272–9.
20. Yehoshua Z, de Amorim Garcia Filho CA, Nunes RP, et al. Comparison of geographic atrophy growth rates using different imaging modalities in the COMPLETE study. Ophthalmic Surg Lasers Imaging Retina 2015;46:413–22.
21. Klein R, Davis MD, Magli YL, et al. The Wisconsin age-related maculopathy grading system. Ophthalmology 1991;98:1128–34.
22. Age-Related Eye Disease Study Research G. The Age-Related Eye Disease Study system for classifying age-related macular degeneration from stereoscopic color fundus photographs: the Age-Related Eye Disease Study Report Number 6. Am J Ophthalmol 2001;132:668–81.
23. Klein ML, Ferris FL 3rd, Armstrong J, et al. Retinal precursors and the development of geographic atrophy in age-related macular degeneration. Ophthalmology 2008;115:1026–31.
24. Complications of Age-related Macular Degeneration Prevention Trial Research G. Risk factors for choroidal neovascularization and geographic atrophy in the complications of age-related macular degeneration prevention trial. Ophthalmology 2008;115:1474–9. 9 e1−6.
25. Klein R, Klein BE, Jensen SC, Meuer SM. The five-year incidence and progression of age-related maculopathy: the Beaver Dam Eye Study. Ophthalmology 1997;104:7–21.
26. Klaver CC, Assink JJ, van Leeuwen R, et al. Incidence and progression rates of age-related maculopathy: the Rotterdam Study. Invest Ophthalmol Vis Sci 2001;42:2237–41.
27. Mitchell P, Wang JJ, Foran S, Smith W. Five-year incidence of age-related maculopathy lesions: the Blue Mountains Eye Study. Ophthalmology 2002;109:1092–7.
28. Pirbhai A, Sheidow T, Hooper P. Prospective evaluation of digital non-stereo color fundus photography as a screening tool in age-related macular degeneration. Am J Ophthalmol 2005;139:455–61.
29. Sunness JS, Bressler NM, Tian Y, et al. Measuring geographic atrophy in advanced age-related macular degeneration. Invest Ophthalmol Vis Sci 1999;40:1761–9.
30. Schmitz-Valckenberg S, Brinkmann CK, Alten F, et al. Semiautomated image processing method for identification and quantification of geographic atrophy in age-related macular degeneration. Invest Ophthalmol Vis Sci 2011;52:7640–6.
31. Ach T, Huisingh C, McGwin G Jr, et al. Quantitative autofluorescence and cell density maps of the human retinal pigment epithelium. Invest Ophthalmol Vis Sci 2014;55:4832–41.
32. Ablonczy Z, Higbee D, Anderson DM, et al. Lack of correlation between the spatial distribution of A2E and lipofuscin fluorescence in the human retinal pigment epithelium. Invest Ophthalmol Vis Sci 2013;54:5535–42.
33. Schmitz-Valckenberg S, Fleckenstein M, Gobel AP, et al. Optical coherence tomography and autofluorescence findings in areas with geographic atrophy due to age-related macular degeneration. Invest Ophthalmol Vis Sci 2011;52:1–6.
34. Sayegh RG, Simader C, Scheschy U, et al. A systematic comparison of spectral-domain optical coherence tomography and fundus autofluorescence in patients with geographic atrophy. Ophthalmology 2011;118:1844–51.
35. Simader C, Sayegh RG, Montuoro A, et al. A longitudinal comparison of spectral−domain optical coherence tomography and fundus autofluorescence in geographic atrophy. Am J Ophthalmol 2014;158:557–566 e1.
36. Moussa K, Lee JY, Stinnett SS, Jaffe GJ. Spectral domain optical coherence tomography-determined morphologic predictors of age-related macular degeneration-associated geographic atrophy progression. Retina 2013;33:1590–9.
37. Lujan BJ, Rosenfeld PJ, Gregori G, et al. Spectral domain optical coherence tomographic imaging of geographic atrophy. Ophthalmic Surg Lasers Imaging 2009;40:96–101.

38. Bearelly S, Chau FY, Koreishi A, et al. Spectral domain optical coherence tomography imaging of geographic atrophy margins. Ophthalmology 2009;116:1762–9.
39. Scholl HP, Peto T, Dandekar S, et al. Inter- and intra-observer variability in grading lesions of age-related maculopathy and macular degeneration. Graefes Arch Clin Exp Ophthalmol 2003;241:39–47.
40. Schmitz-Valckenberg S, Fleckenstein M, Gobel AP, et al. Evaluation of autofluorescence imaging with the scanning laser ophthalmoscope and the fundus camera in age-related geographic atrophy. Am J Ophthalmol 2008;146:183–92.
41. Yehoshua Z, Garcia Filho CA, Penha FM, et al. Comparison of geographic atrophy measurements from the OCT fundus image and the sub-RPE slab image. Ophthalmic Surg Lasers Imaging Retina 2013;44:127–32.
42. Chen Q, de Sisternes L, Leng T, et al. Semi-automatic geographic atrophy segmentation for SD-OCT images. Biomed Opt Express 2013;4:2729–50.
43. Feuer WJ, Yehoshua Z, Gregori G, et al. Square root transformation of geographic atrophy area measurements to eliminate dependence of growth rates on baseline lesion measurements: a reanalysis of Age-Related Eye Disease Study report no. 26. JAMA Ophthalmol 2013;131:110–1.
44. Yehoshua Z, de Amorim Garcia Filho CA, Nunes RP, et al. Systemic complement inhibition with eculizumab for geographic atrophy in age-related macular degeneration: the COMPLETE study. Ophthalmology 2014;121:693–701.
45. Nunes RP, Gregori G, Yehoshua Z, et al. Predicting the progression of geographic atrophy in age-related macular degeneration with SD-OCT en face imaging of the outer retina. Ophthalmic Surg Lasers Imaging Retina 2013;44:344–59.
46. Stetson PF, Yehoshua Z, Garcia Filho CA, et al. OCT minimum intensity as a predictor of geographic atrophy enlargement. Invest Ophthalmol Vis Sci 2014;55:792–800.
47. Bird AC, Phillips RL, Hageman GS. Geographic atrophy: a histopathological assessment. JAMA Ophthalmol 2014;132:338–45.
48. Domalpally A, Danis RP, White J, et al. Circularity index as a risk factor for progression of geographic atrophy. Ophthalmology 2013;120:2666–71.
49. Zhang K, Hopkins JJ, Heier JS, et al. Ciliary neurotrophic factor delivered by encapsulated cell intraocular implants for treatment of geographic atrophy in age-related macular degeneration. Proc Natl Acad Sci U S A 2011;108:6241–5.
50. Wong WT, Kam W, Cunningham D, et al. Treatment of geographic atrophy by the topical administration of OT-551: results of a phase II clinical trial. Invest Ophthalmol Vis Sci 2010;51:6131–9.
51. Mata NL, Lichter JB, Vogel R, et al. Investigation of oral fenretinide for treatment of geographic atrophy in age-related macular degeneration. Retina 2013;33:498–507.
52. Wong WT, Dresner S, Forooghian F, et al. Treatment of geographic atrophy with subconjunctival sirolimus: results of a phase I/II clinical trial. Invest Ophthalmol Vis Sci 2013;54:2941–50.
53. Yehoshua Z, Wang F, Rosenfeld PJ, et al. Natural history of drusen morphology in age-related macular degeneration using spectral domain optical coherence tomography. Ophthalmology 2011;118:2434–41.
54. Davis MD, Gangnon RE, Lee LY, et al. The Age-Related Eye Disease Study severity scale for age-related macular degeneration: AREDS Report No. 17. Arch Ophthalmol 2005;123:1484–98.
55. Wang JJ, Foran S, Smith W, Mitchell P. Risk of age-related macular degeneration in eyes with macular drusen or hyperpigmentation: the Blue Mountains Eye Study cohort. Arch Ophthalmol 2003;121:658–63.
56. Klein R, Klein BE, Tomany SC, et al. Ten-year incidence and progression of age-related maculopathy: the Beaver Dam Eye Study. Ophthalmology 2002;109:1767–79.
57. Klein R, Klein BE, Knudtson MD, et al. Fifteen-year cumulative incidence of age-related macular degeneration: the Beaver Dam Eye Study. Ophthalmology 2007;114:253–62.
58. Wang JJ, Rochtchina E, Lee AJ, et al. Ten-year incidence and progression of age-related maculopathy: the Blue Mountains Eye Study. Ophthalmology 2007;114:92–8.
59. Ferris FL, Davis MD, Clemons TE, et al. A simplified severity scale for age-related macular degeneration: AREDS Report No. 18. Arch Ophthalmol 2005;123:1570–4.
60. Seddon JM, Sharma S, Adelman RA. Evaluation of the clinical age-related maculopathy staging system. Ophthalmology 2006;113:260–6.
61. Bird AC, Bressler NM, Bressler SB, et al. An international classification and grading system for age-related maculopathy and age-related macular degeneration. The International ARM Epidemiological Study Group. Surv Ophthalmol 1995;39:367–74.
62. Bressler NM, Munoz B, Maguire MG, et al. Five-year incidence and disappearance of drusen and retinal pigment epithelial abnormalities. Waterman study. Arch Ophthalmol 1995;113:301–8.
63. Sparrow JM, Dickinson AJ, Duke AM, et al. Seven year follow-up of age-related maculopathy in an elderly British population. Eye (Lond) 1997;11(Pt 3):315–24.
64. Bartlett H, Eperjesi F. Use of fundus imaging in quantification of age-related macular change. Surv Ophthalmol 2007;52:655–71.
65. Smith RT, Chan JK, Nagasaki T, et al. A method of drusen measurement based on reconstruction of fundus background reflectance. Br J Ophthalmol 2005;89:87–91.
66. Friberg TR, Huang L, Palaiou M, Bremer R. Computerized detection and measurement of drusen in age-related macular degeneration. Ophthalmic Surg Lasers Imaging 2007;38:126–34.
67. Peli E, Lahav M. Drusen measurement from fundus photographs using computer image analysis. Ophthalmology 1986;93:1575–80.
68. Morgan WH, Cooper RL, Constable IJ, Eikelboom RH. Automated extraction and quantification of macular drusen from fundal photographs. Aust N Z J Ophthalmol 1994;22:7–12.
69. Zweifel SA, Spaide RF, Curcio CA, et al. Reticular pseudodrusen are subretinal drusenoid deposits. Ophthalmology 2010;117:303–12 e1.
70. Spaide RF. Colocalization of pseudodrusen and subretinal drusenoid deposits using high-density en face spectral domain optical coherence tomography. Retina 2014;34:2336–45.
71. Curcio CA, Messinger JD, Sloan KR, et al. Subretinal drusenoid deposits in non-neovascular age-related macular degeneration: morphology, prevalence, topography, and biogenesis model. Retina 2013;33:265–76.
72. Schaal KB, Legarreta AD, Gregori G, et al. Widefield en face optical coherence tomography imaging of subretinal drusenoid deposits. Ophthalmic Surg Lasers Imaging Retina 2015;46:550–9.
73. Sarks SH, Arnold JJ, Killingsworth MC, Sarks JP. Early drusen formation in the normal and aging eye and their relation to age related maculopathy: a clinicopathological study. Br J Ophthalmol 1999;83:358–68.

74. Gregori G, Wang F, Rosenfeld PJ, et al. Spectral domain optical coherence tomography imaging of drusen in nonexudative age-related macular degeneration. Ophthalmology 2011;118:1373–9.
75. Ouyang Y, Heussen FM, Hariri A, et al. Optical coherence tomography-based observation of the natural history of drusenoid lesion in eyes with dry age-related macular degeneration. Ophthalmology 2013;120:2656–65.
76. Wu Z, Luu CD, Ayton LN, et al. Optical coherence tomography-defined changes preceding the development of drusen-associated atrophy in age-related macular degeneration. Ophthalmology 2014;121:2415–22.
77. Chen Q, Leng T, Zheng LL, et al. An improved optical coherence tomography-derived fundus projection image for drusen visualization. Retina 2014;34:996–1005.
78. Folgar FA, Yuan EL, Sevilla M, et al. Drusen volume and retinal pigment epithelium abnormal thinning volume predict 2-year progression of age-related macular degeneration. Ophthalmology 2016;123:39–50.e1.
79. Schlanitz FG, Sacu S, Baumann B, et al. Identification of drusen characteristics in age-related macular degeneration by polarization-sensitive optical coherence tomography. Am J Ophthalmol 2015;160:335–344.e1.
80. Gregori G, Yehoshua Z, Garcia Filho CA, et al. Change in drusen area over time compared using spectral-domain optical coherence tomography and color fundus imaging. Invest Ophthalmol Vis Sci 2014;55:7662–8.
81. Yehoshua Z, Gregori G, Sadda SR, et al. Comparison of drusen area detected by spectral domain optical coherence tomography and color fundus imaging. Invest Ophthalmol Vis Sci 2013;54:2429–34.
82. Diniz B, Ribeiro R, Heussen FM, et al. Drusen measurements comparison by fundus photograph manual delineation versus optical coherence tomography retinal pigment epithelial segmentation automated analysis. Retina 2014;34:55–62.
83. de Sisternes L, Simon N, Tibshirani R, et al. Quantitative SD-OCT imaging biomarkers as indicators of age-related macular degeneration progression. Invest Ophthalmol Vis Sci 2014;55:7093–103.
84. Nathoo NA, Or C, Young M, et al. Optical coherence tomography-based measurement of drusen load predicts development of advanced age-related macular degeneration. Am J Ophthalmol 2014;158:757–61 e1.
85. Jain N, Farsiu S, Khanifar AA, et al. Quantitative comparison of drusen segmented on SD-OCT versus drusen delineated on color fundus photographs. Invest Ophthalmol Vis Sci 2010;51:4875–83.
86. Schlanitz FG, Ahlers C, Sacu S, et al. Performance of drusen detection by spectral-domain optical coherence tomography. Invest Ophthalmol Vis Sci 2010;51:6715–21.
87. Baumann B, Gotzinger E, Pircher M, et al. Segmentation and quantification of retinal lesions in age-related macular degeneration using polarization-sensitive optical coherence tomography. J Biomed Opt 2010;15:061704.
88. Gotzinger E, Pircher M, Geitzenauer W, et al. Retinal pigment epithelium segmentation by polarization sensitive optical coherence tomography. Opt Express 2008;16:16410–22.
89. Schlanitz FG, Baumann B, Spalek T, et al. Performance of automated drusen detection by polarization-sensitive optical coherence tomography. Invest Ophthalmol Vis Sci 2011;52:4571–9.
90. Khanifar AA, Koreishi AF, Izatt JA, Toth CA. Drusen ultrastructure imaging with spectral domain optical coherence tomography in age-related macular degeneration. Ophthalmology 2008;115:1883–90.
91. Stopa M, Bower BA, Davies E, et al. Correlation of pathologic features in spectral domain optical coherence tomography with conventional retinal studies. Retina 2008;28:298–308.
92. Chew EY, Clemons TE, Agron E, et al. Ten-year follow-up of age-related macular degeneration in the Age-Related Eye Disease Study: AREDS report no. 36. JAMA Ophthalmol 2014;132:272–7.
93. Cukras C, Agron E, Klein ML, et al. Natural history of drusenoid pigment epithelial detachment in age-related macular degeneration: Age-Related Eye Disease Study Report No. 28. Ophthalmology 2010;117:489–99.
94. Parodi MB, Virgili G, Evans JR. Laser treatment of drusen to prevent progression to advanced age-related macular degeneration. Cochrane Database Syst Rev 2009;(3):CD006537.
95. Abdelsalam A, Del Priore L, Zarbin MA. Drusen in age-related macular degeneration: pathogenesis, natural course, and laser photocoagulation-induced regression. Surv Ophthalmol 1999;44:1–29.
96. Margolis R, Ober MD, Freund KB. Disappearance of drusen after rhegmatogenous retinal detachment. Retin Cases Brief Rep 2010;4:254–6.
97. Dithmar S, Pollithy S, Ach T. Disappearance of central confluent soft drusen following vitrectomy and ILM peeling. Eye (Lond) 2013;27:779–81.
98. Fuseya M, Imamura Y, Ishida S, et al. Regression of macular drusen after pars plana vitrectomy in a patient with age-related macular degeneration. Retin Cases Brief Rep 2007;1:160–2.
99. Krishnan R, Lochhead J. Regression of soft drusen and drusenoid pigment epithelial detachment following intravitreal anti-vascular endothelial growth factor therapy. Can J Ophthalmol 2010;45:83–4.
100. Jobling AI, Guymer RH, Vessey KA, et al. Nanosecond laser therapy reverses pathologic and molecular changes in age-related macular degeneration without retinal damage. FASEB J 2015;29:696–710.
101. Guymer RH, Brassington KH, Dimitrov P, et al. Nanosecond-laser application in intermediate AMD: 12-month results of fundus appearance and macular function. Clin Experiment Ophthalmol 2014;42:466–79.
102. Lavinsky D, Palanker D. Nondamaging photothermal therapy for the retina: initial clinical experience with chronic central serous retinopathy. Retina 2015;35:213–22.
103. Lavinsky D, Sramek C, Wang J, et al. Subvisible retinal laser therapy: titration algorithm and tissue response. Retina 2014;34:87–97.
104. de Amorim Garcia Filho CA, Yehoshua Z, Gregori G, et al. Change in drusen volume as a novel clinical trial endpoint for the study of complement inhibition in age-related macular degeneration. Ophthalmic Surg Lasers Imaging Retina 2014;45:18–31.
105. Garcia Filho CA, Yehoshua Z, Gregori G, et al. Change in drusen volume as a novel clinical trial endpoint for the study of complement inhibition in age-related macular degeneration. Ophthalmic Surg Lasers Imaging Retina 2014;45:18–31.
106. Chavali VR, Diniz B, Huang J, et al. Association of OCT derived drusen measurements with AMD associated-genotypic SNPs in Amish population. J Clin Med 2015;4:304–17.
107. Busse JW, Bhandari M, Ferreira-Gonzalez I, et al. Use and interpretation of composite end points in orthopaedic trials. J Bone Joint Surg Am 2012;94(Suppl 1):65–9.
108. Tomlinson G, Detsky AS. Composite end points in randomized trials: there is no free lunch. JAMA 2010;303:267–8.

Footnotes and Financial Disclosures

Originally received: October 20, 2015.
Final revision: January 11, 2016.
Accepted: January 21, 2016.
Available online: March 5, 2016. Manuscript no. 2015-1837.

Department of Ophthalmology, Bascom Palmer Eye Institute, University of Miami Miller School of Medicine, Miami, Florida.

Financial Disclosure(s):
The author(s) have made the following disclosure(s): K.B.S.: Funding – the DFG (German Research Foundation) Grant SCHA 1869/1-1.

P.J.R. and G.G.: Research support – Carl Zeiss Meditec, Inc.

G.G. and the University of Miami co-own a patent that is licensed to Carl Zeiss Meditec, Inc.

P.J.R. and Z.Y.: Research support – Acucela and Apellis.

P.J.R.: Research support – Genentech/Roche, GlaxoSmithKline, Neurotech, Ocata Therapeutics, and Tyrogenex; Consultant – Achillion, Acucela, Alcon, Bayer, Chengdu Kanghong Biotech, CoDa Therapeutics, Genentech/Roche, Healios K.K., Merck, Regeneron, Stealth, and Tyrogenex.

W.J.F.: Grants – National Eye Institute, Research to Prevent Blindness, and Department of Defense.

Author Contributions:

Conception and design: Schaal, Rosenfeld, Gregori, Yehoshua, Feuer

Data collection: Schaal, Rosenfeld, Gregori, Yehoshua, Feuer

Analysis and interpretation: Schaal, Rosenfeld, Gregori, Yehoshua, Feuer

Obtained funding: Not applicable

Overall responsibility: Schaal, Rosenfeld, Gregori, Yehoshua, Feuer

Abbreviations and Acronyms:
AMD = age-related macular degeneration; **AREDS** = Age-Related Eye Disease Study; **BM** = Bruch's membrane; **CFH** = complement factor H; **CFP** = color fundus photography; **CI** = circularity index; **EpM** = Endpoint Management; **FAF** = fundus autofluorescence; **GA** = geographic atrophy; **iAMD** = intermediate age-related macular degeneration; **MNV** = macular neovascularization; **OCT** = optical coherence tomography; **OFI** = OCT fundus image; **PS-OCT** = polarization-sensitive optical coherence tomography; **RPE** = retinal pigment epithelium; **SD OCT** = spectral-domain optical coherence tomography; **VEGF** = vascular endothelial growth factor.

Correspondence:
Philip J. Rosenfeld, MD, PhD, Bascom Palmer Eye Institute, 900 NW 17th Street, Miami, FL 33136. E-mail: prosenfeld@med.miami.edu.